LAWRENCE
LIVERMORE
NATIONAL
LABORATORY

LLNL-TR-653675

THERMODYNAMIC ASSESSMENT OF THE TERNARY ALLOY SYSTEM LI-SN-ZN

P. E. Turchi

April 24, 2014

Disclaimer

This document was prepared as an account of work sponsored by an agency of the United States government. Neither the United States government nor Lawrence Livermore National Security, LLC, nor any of their employees makes any warranty, expressed or implied, or assumes any legal liability or responsibility for the accuracy, completeness, or usefulness of any information, apparatus, product, or process disclosed, or represents that its use would not infringe privately owned rights. Reference herein to any specific commercial product, process, or service by trade name, trademark, manufacturer, or otherwise does not necessarily constitute or imply its endorsement, recommendation, or favoring by the United States government or Lawrence Livermore National Security, LLC. The views and opinions of authors expressed herein do not necessarily state or reflect those of the United States government or Lawrence Livermore National Security, LLC, and shall not be used for advertising or product endorsement purposes.

This work performed under the auspices of the U.S. Department of Energy by Lawrence Livermore National Laboratory under Contract DE-AC52-07NA27344.

THERMODYNAMIC ASSESSMENT OF THE TERNARY ALLOY SYSTEM Li-Sn-Zn

LDRD-ENG-14-ER-035 Report
April 14, 2014

P. E. A. Turchi <Turchi1@llnl.gov>

Lawrence Livermore National Laboratory, Physical and Life Sciences Directorate, L-352, P. O. Box 808, Livermore CA 94551

Project Objective

The goal of this project is to predict thermodynamics and structure-properties relationships of a series of Li-based alloys for the development of advanced tritium breeding materials that exhibit the beneficial properties of pure lithium while mitigating its chemical reactivity issues for fusion applications. This project makes use of phenomenological thermodynamics based on the CALPHAD (CALculation of PHAse Diagrams), and the use of the Thermo-Calc software (see Appendix A), and experimental calorimetric data and structural characterization for the purpose of validating the data. The initial selection of Sn and Zn as solutes is considered in this first report. Originally Li-Sn alloys have shown promise in meeting tritium breeding ratio (TBR) and energy multiplication requirements. However with the addition of Zn, we expect an improvement in the nuclear, thermal, and chemical requirements of the working fluid. Other substitutes will be considered once neutronic calculations are carried out.

Hence the objective of this first task is to carry out a thermodynamic assessment of the Li-Sn-Zn alloy system, as part of the development of a self-consistent and validated thermodynamic database that will include other solute elements for optimizing the properties of blanket materials in fusion-based reactors. This obviously involves the thermodynamic assessment of the three binary subsystems, namely Li-Sn, Li-Zn, and Sn-Zn.

I. Thermodynamic assessment of the three binary, Li-Sn, Li-Zn, and Sn-Zn alloy systems

The crystal structure data for the two binaries, Li-Sn and Li-Zn is shown in Table I, whereas for Sn-Zn, no other phases than those associated with the pure elements Sn and Zn exist.

Li-Sn Crystal Structure Data

Phase	Composition, at.% Sn	Pearson symbol	Space group	Struktur-bericht designation	Prototype
(Li)	0	*cI*2	$Im\bar{3}m$	*A*2	W
$Li_{22}Sn_5$	18.5	*cF*432	*F*23	...	...
Li_7Sn_2	22.2 to ?	*oC*36	*Cmmm*	...	...
$Li_{13}Sn_5$	27.8	*hP*18	$P\bar{3}m1$	...	...
Li_5Sn_2	28.6	*hR*7	$R\bar{3}m$	$D8_i$	Mo_2B_5
Li_7Sn_3	30	*mP*20	$P2_1/m$	...	...
LiSn	50	*mP*6	*P*2/*m*	...	...
Li_2Sn_5	71.4	*tI*14	*P*4/*mbm*	...	...
(βSn)	100	*tI*4	$I4_1/amd$	*A*5	βSn
(αSn)	100	*cF*8	$Fd\bar{3}m$	*A*4	C(diamond)

Li-Zn Crystal Structure Data

Phase	Composition, at.% Zn	Pearson symbol	Space group	Struktur-bericht designation	Prototype
(αLi)(a)	0	*hP*2	*P*6$_3$/*mmc*	*A*3	Mg
(βLi)	0 to 1.5	*cI*2	*Im*$\bar{3}$*m*	*A*2	W
LiZn	~50 to 54	*cF*16	*Fd*$\bar{3}$*m*	*B*32	NaTl
αLi$_2$Zn$_3$	~58 to 60	*c***?	...	...	...
βLi$_2$Zn$_3$.....	~50 to 67	...	...	...	...
LiZn$_2$	66.7	...	...	...	...
αLi$_2$Zn$_5$(b).....	~70 to 73	*h***(c)	...	...	...
βLi$_2$Zn$_5$(b)	71 to 92	...	...	...	...
βLiZn$_4$	~75 to 90	*hP*2	*P*6$_3$/*mmc*(d)	...	...
αLiZn$_4$	~77 to 85	*h***(e)	...	...	...
(Zn)	100	*hP*2	*P*6$_3$/*mmc*	*A*3	Mg

Table I. Crystal structure data for Li-Sn (top) and Li-Zn alloys (bottom).

The known phase diagrams of the three binary systems from Ref. [1] are shown in Fig. 1.

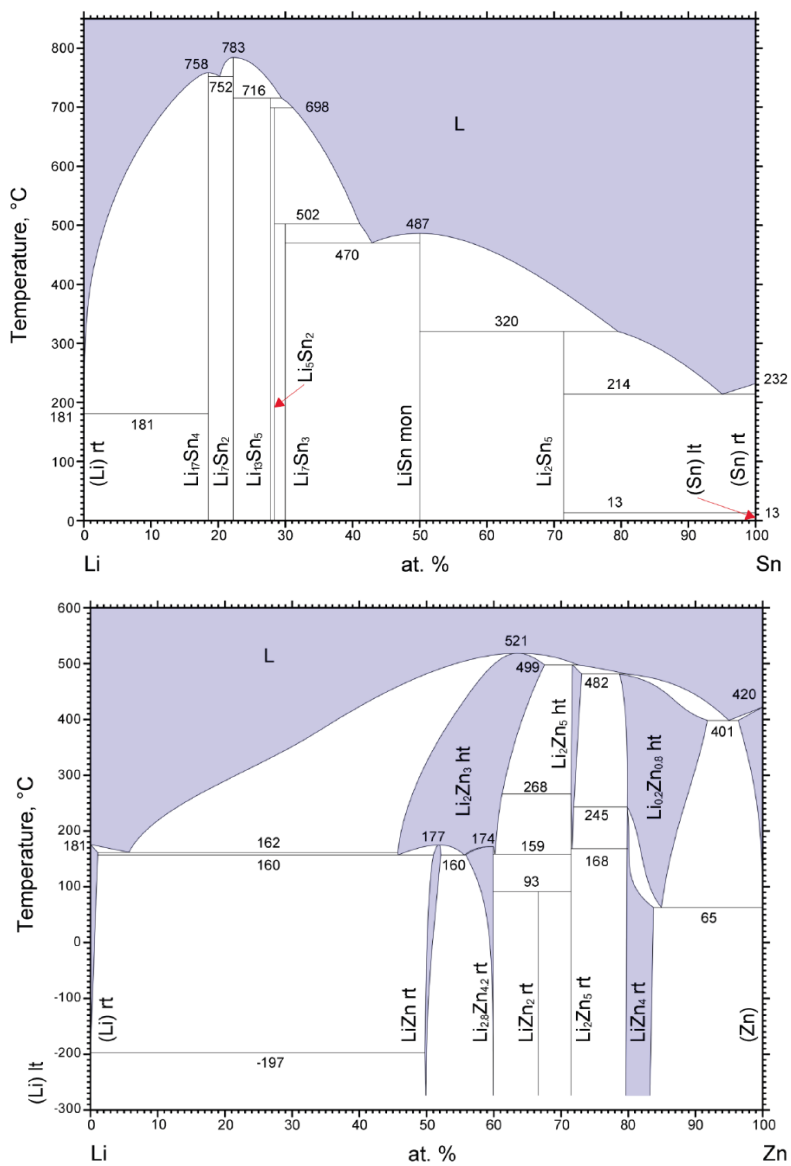

Figure 1. Assessed phase diagrams according to: Sangster and Bale [2] for Li-Sn (top), Liang *et al*. [3] for Li-Zn (middle), and Doi *et al*. [4] for Sn-Zn (bottom). All three phase diagrams are taken from Ref. [1].

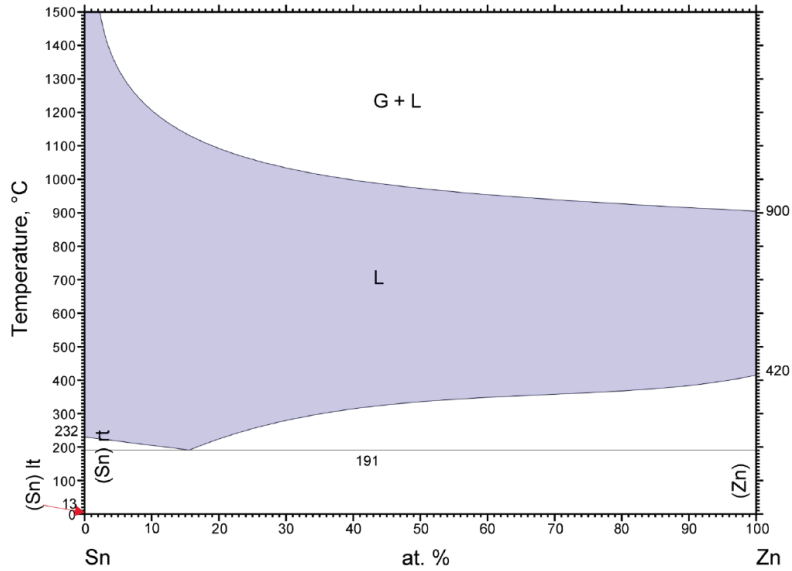

In the case of Li-Sn, a newest version of the phase diagram was proposed in 2006, and is shown in Fig. 2.

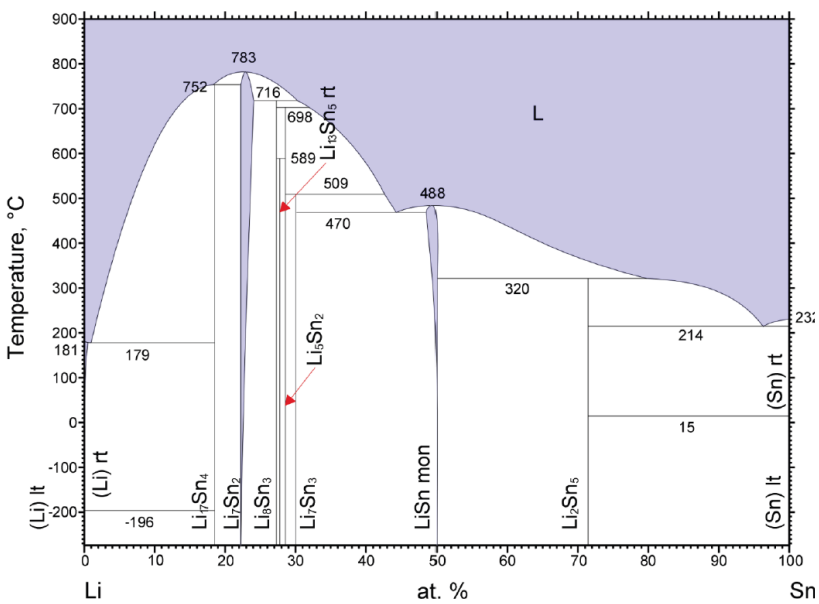

Figure 2. Assessed Li-Sn phase diagrams according to: Du *et al*. [5]. The phase diagram is taken from Ref. [1].

Regarding the pure elements the melting points reported in Table 2 show that Li has the lowest melting point, which explain why Li has been the favored materials for fusion blanket.

Element	Melting Point (°C)	Ground-state Structure
Li	181	β: bcc, A2 (α: hcp, A3)
Sn	232	β: bct, A5 (α: diamond, A4)
Zn	420	hcp, A3

Table II. Melting point of the pure elements Li, Sn, and Zn (Cf. Appendix C for more details).

However since Li is highly chemically reactive with air, water, and other compounds, alloying seems to be a legitimate route to reduce the chemical reactivity. The addition of Sn would improve the properties of Li, although, as shown in the phase diagram displayed in Fig. 1 (top), in the highly Li-rich region of the phase diagram, very stable compounds, $Li_{17}Sn_4$, Li_7Sn_2, $Li_{13}Sn_5$, Li_5Sn_2, and Li_7Sn_3 form: the first two transform congruently into the liquid phase at high temperature (758 and 783 ºC) whereas the other three compounds go through eutectoid or eutectic reactions, also at much higher temperatures than the melting temperature of Li. Since the phase diagram of Sn-Zn, see Fig. 1 (bottom) only displays a simple eutectic reaction at 191 ºC, close to the melting point of Li, and the Li-Zn phase diagram, see Fig. 1 (middle), shows an eutectic reaction at 162 ºC and about 5 at. % Zn, below the melting point of Li, a possibility exists that the combination of Sn and Zn in Li may satisfy the requirements, and at the same time maintains a low melting point in an optimum composition range of the Li-rich ternary alloy.

An extensive literature search has been done on available thermodynamic assessments for these three alloy systems. For Li-Sn, a thermodynamic optimization has been proposed by Du *et al*. in 2006 [5], and experimental thermodynamic data by Knudsen effusion mass spectrometry by Henriques *et al*. have been reported in 2014 [6]. For Li-Zn, only one thermodynamic assessment has been performed by Liang *et al*. in 2008 [7] that has been used in the assessment of the ternary system Al-Li-Zn in 2011 by Guo *et al*. [8]. Finally for Sn-Zn, several assessments have been performed in the context on thermodynamic studies of ternary system: 1) Ohtani *et al*. in the case of Sn-Ag-Zn in 1999 [9]; 2), Cui *et al*. in the cased of In-Sn-Zn in 2001 [10]; 3) Doi *et al*. in the case of Sn-Ti-Zn in 2006 [4]; 4) Vizdal *et al*. in the case of Bi-Sn-Zn in 2007 [11]; 5) Yang *et al*. in the case of Sn-Bi-Zn in 2008 [12]; 6) Huang *et al*. in the case of Sn-Zn-Cu in 2009 [13]; and 7) Vassilev et al. in the case of Ag-Sn-Zn [14].

A critical analysis of the available data led to the following selecting to build up the thermodynamic database for the three binary subsystems that make up the ternary Li-Sn-Zn as reported in Table III

Binary Alloy	Authors	Year	Reference #
Li-Sn	Du *et al*.	2006	[5]
Li-Zn	Liang *et al*.	2008	[7]
Sn-Zn	Huang *et al*.	2009	[13]

Table III. Thermodynamic data selection for the three binary subsystems, Li-Sn, Li-Zn, and Sn-Zn.

Some modifications have been made to the thermodynamic data to make the Gibbs energy models compatible among the three binary alloys, and also correct some artifacts generated with the proposed data.

In terms of thermodynamic modeling for the Gibbs energy for each phase of the three alloy systems the following has to be considered:

Li-Sn: the liquid and LiSn are treated as solution phases whereas $Li_{17}Sn_4$, Li_7Sn_2, $Li_{13}Sn_5$, Li_5Sn_2, Li_7Sn_3, and Li_2Sn_5 are treated as compounds.

Li-Zn: the liquid, bcc (A2), hcp (A3), LiZn, Li_2Zn_3, Li_2Zn_5, and $LiZn_4$ are treated as solid solutions whereas Li_9Zn_4, and Li_3Zn_2 are treated as compounds.

Sn-Zn: the liquid, bct (A5), and hcp are treated as solid solutions.

The current thermodynamic database is given in Appendix B, and the thermodynamically assessed equilibrium phase diagrams of the three binary subsystems Li-Sn, Li-Zn, and Sn-Zn, based on the CALPHAD methodology, are given in Figs. 3, 4, and 5, respectively.

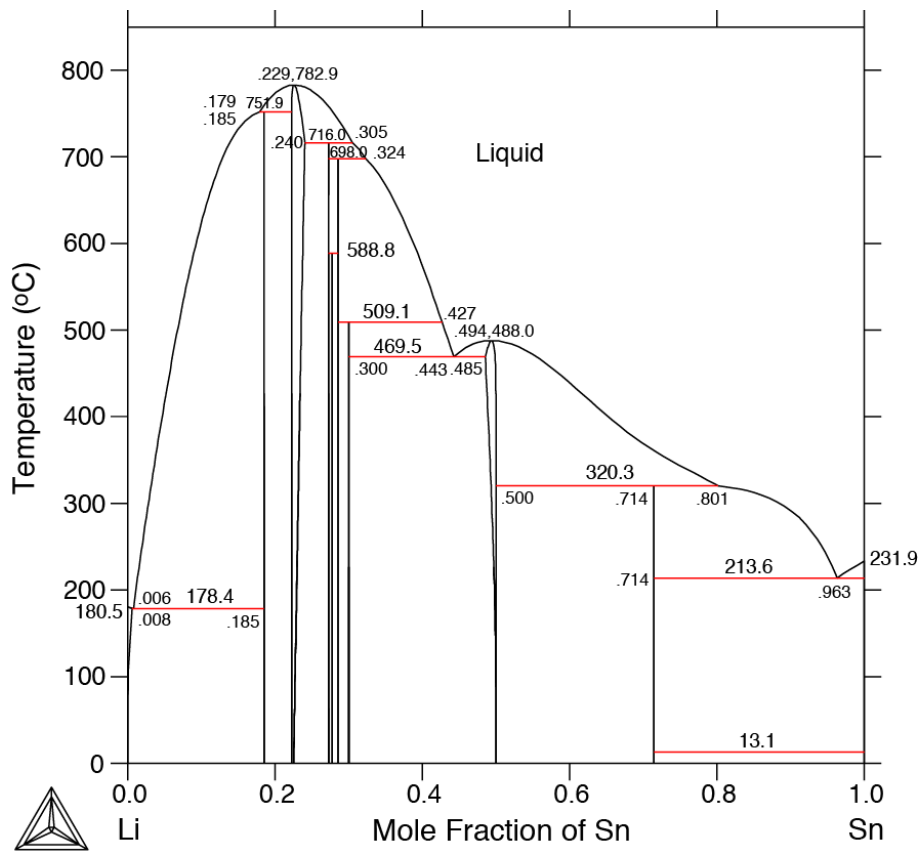

Figure 3. CALPHAD assessment of the Li-Sn phase diagram.

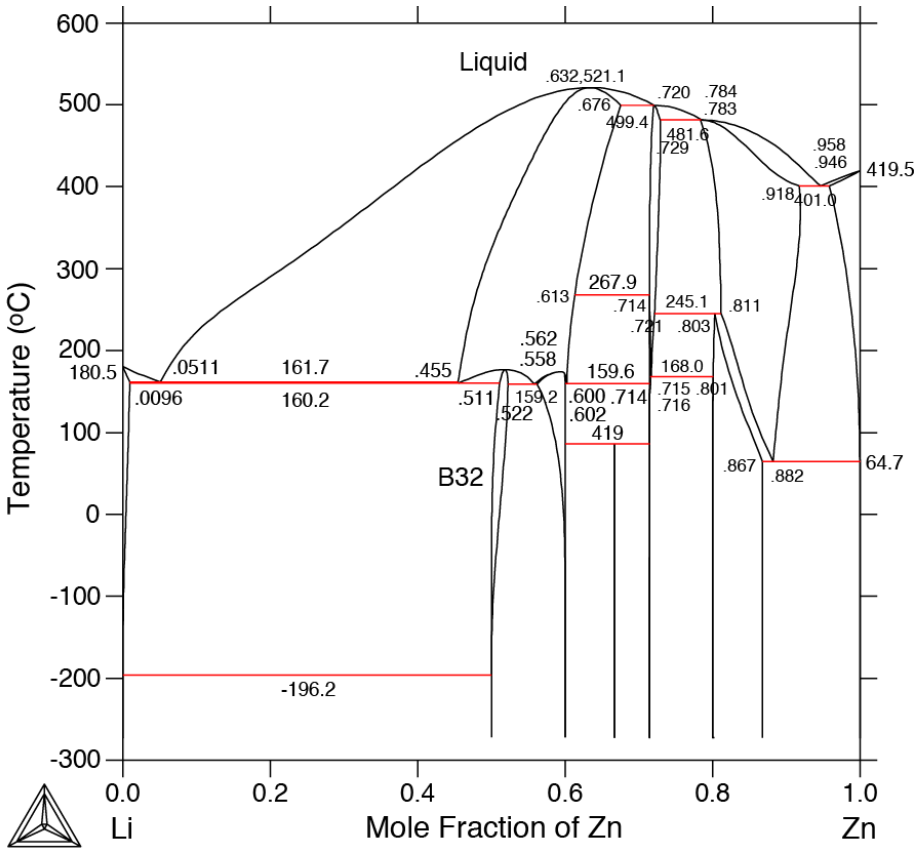

Figure 4. CALPHAD assessment of the Li-Zn phase diagram.

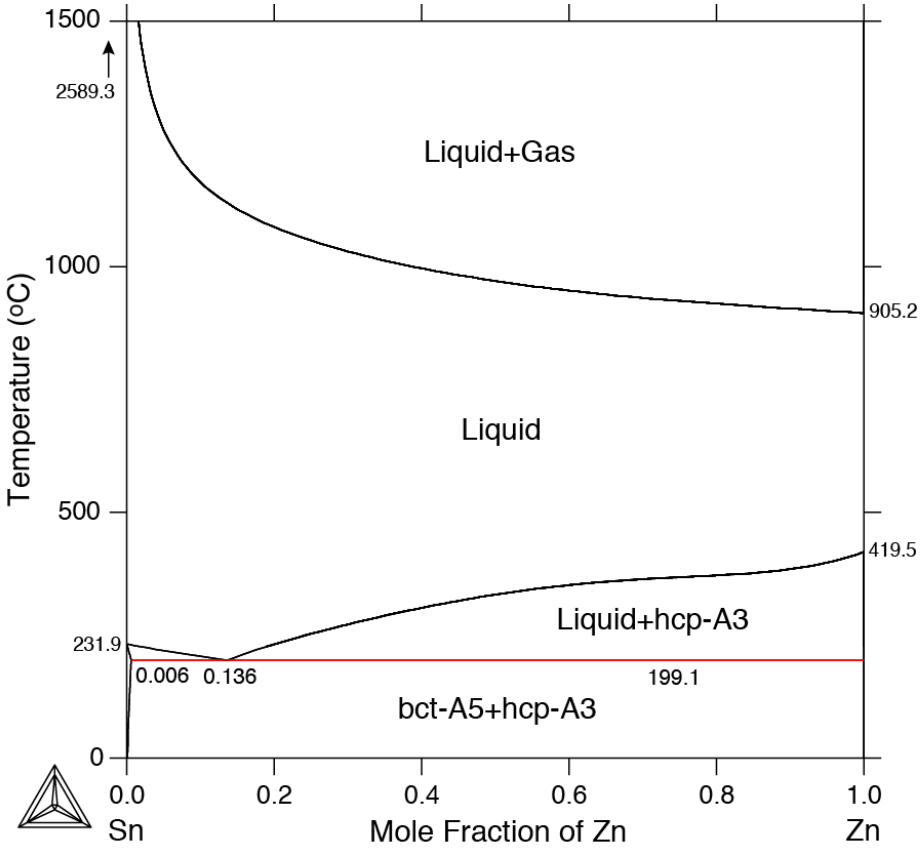

Figure 5. CALPHAD assessment of the Sn-Zn phase diagram.

II. CALPHAD-based thermodynamic modeling of the Li-Sn-Zn phase diagram

The thermodynamic data of three binaries, Li-Sn, Li-Zn, and Sn-Zn, have been put together in a consistent way, see Appendix B, to calculate isothermal sections of the ternary Li-Sn-Zn alloy system. At this point, since no experimental data are available for this ternary alloy system at any composition, it was assumed that no ternary compounds were formed, and that there was no contribution to the excess Gibbs energy, ${}^{\Phi}G^{xs}_{mix}$, of any phase (solid, liquid, or gas), given by Eq. A6 of Appendix A, coming from a ternary interaction ${}^{\phi}L_{IJK}$ that would lead to the following extra contribution:

$${}^{\Phi}G_{IJK} = c_I c_J c_K \, {}^{\phi}L_{IJK}$$

It is worth noting that there is little evidence for the need for interaction terms of any higher order than this, and prediction of the thermodynamic properties of substitutional solution phases in multi-component alloys is usually based on an assessment of binary **and** ternary terms.

The isothermal sections of the ternary phase diagram are given in the Muggianu representation [15], which is the most common one used for describing the thermodyanmics of multi-component alloys, and the results are shown in Fig. 6.

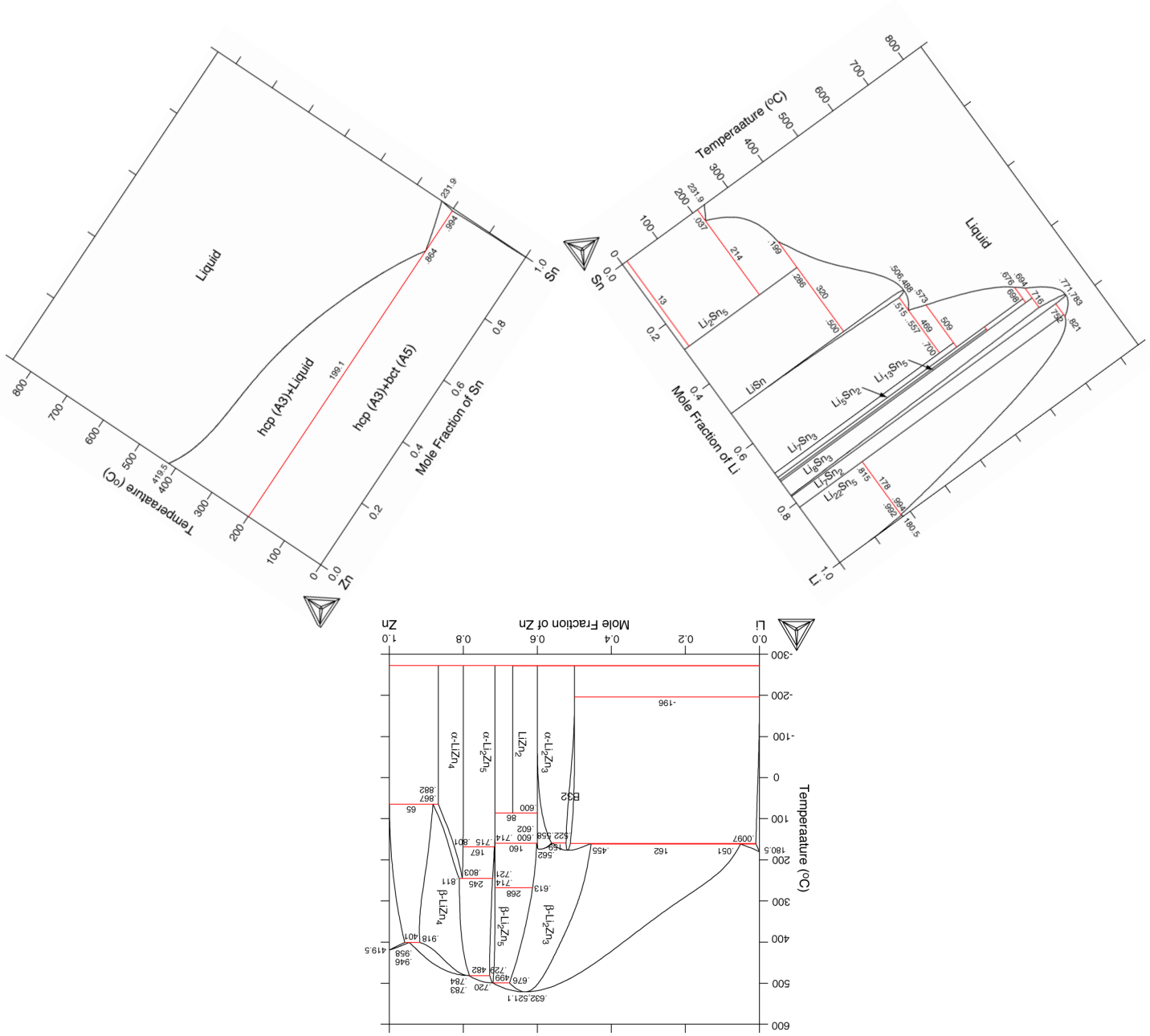

Figure 6. Summary of the thermodynamis in terms of binary phase diagram data for Li-Sn, Li-Zn, and Sn-Zn that are used to predict the phase properties in the ternary Li-Sn-Zn alloy system.

In the following the predicted phase diagram of the ternary Li-Sn-Zn system is presented with: first a few isothermal sections in the high Li-content corner of the phase diagram at various temperatures, see Figs. 7 and 8; second, two isothermal sections at 973 K (700 ºC) and 673 K (400 ºC), see Fig. 9; and third the predicted liquidus surface at high Li-content for the ternary Li-Sn-Zn alloy system, see Fig. 10.

1173 / 1073 K

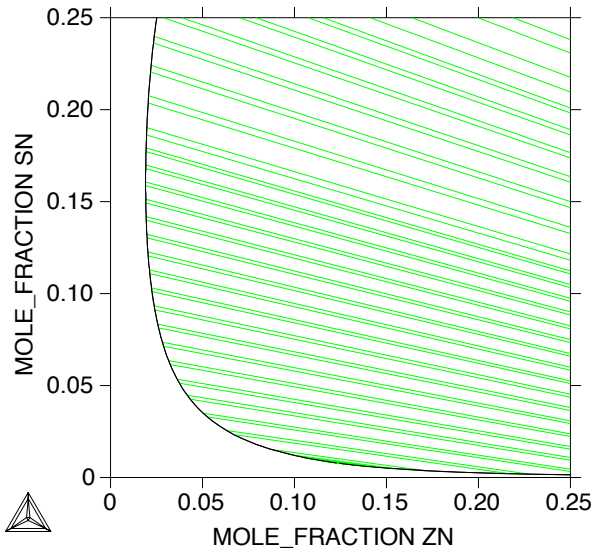

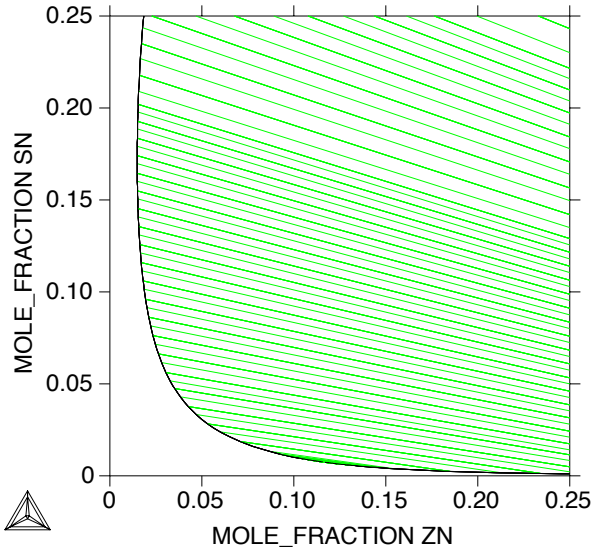

1023 / 973 K

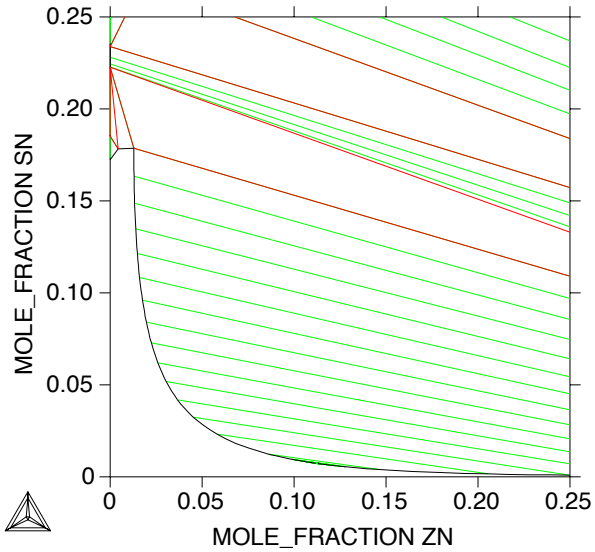

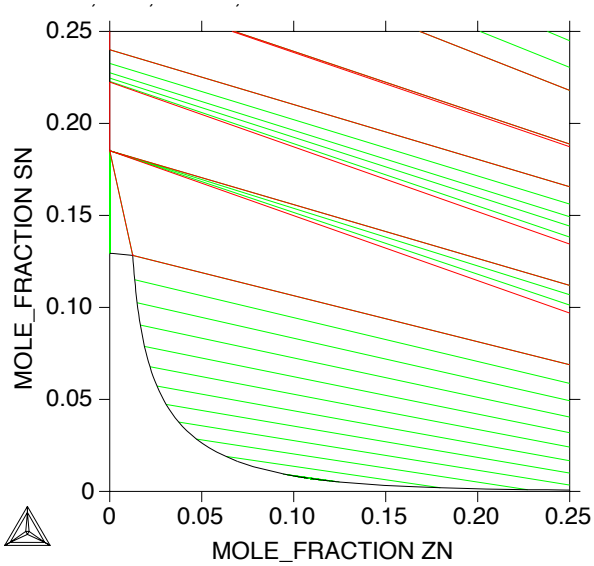

873 / 773 K

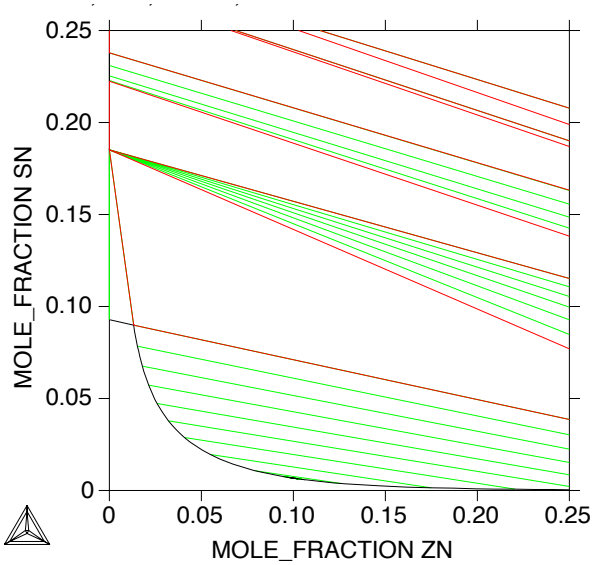

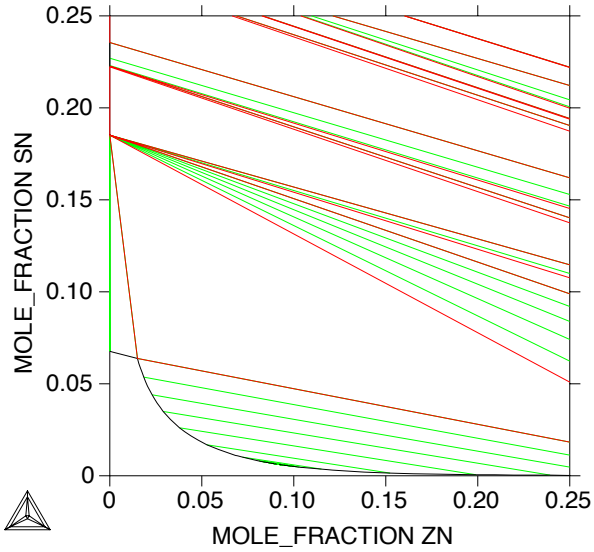

673 / 653 K

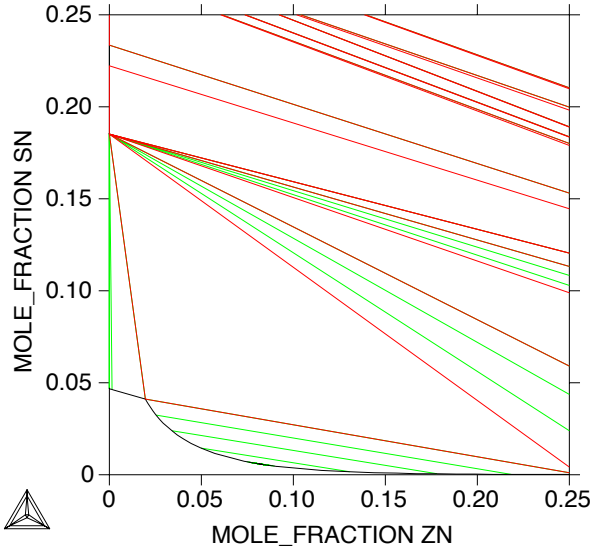

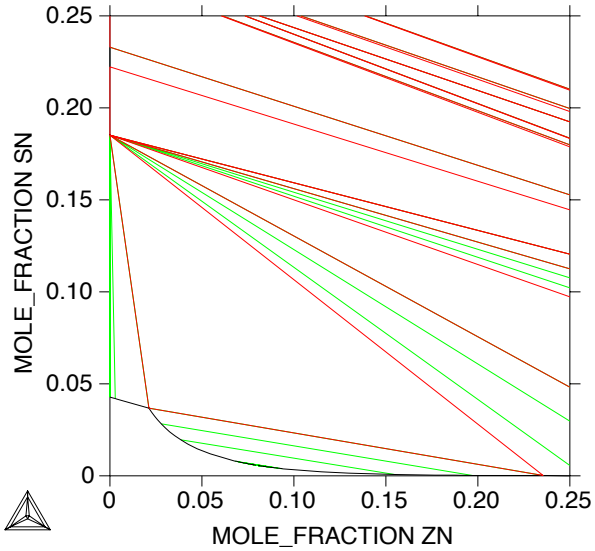

633 / 623 K

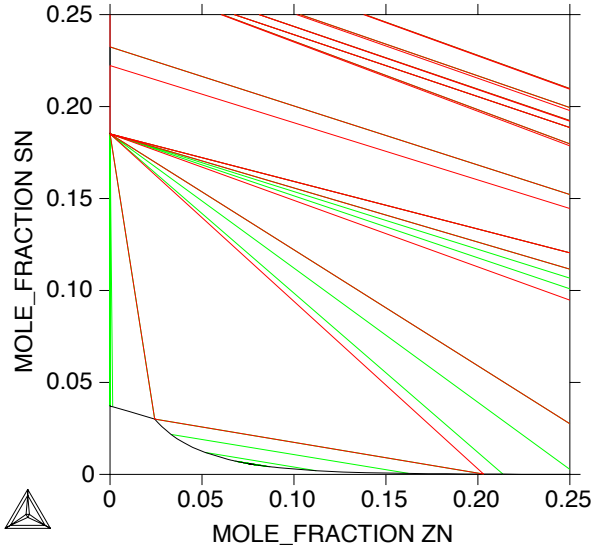

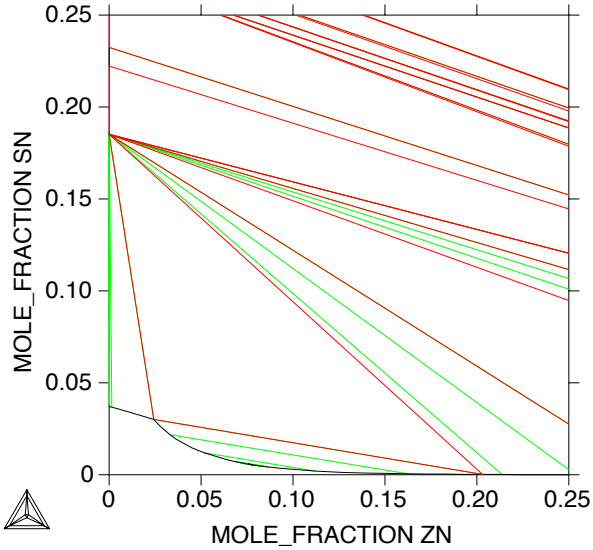

573 K

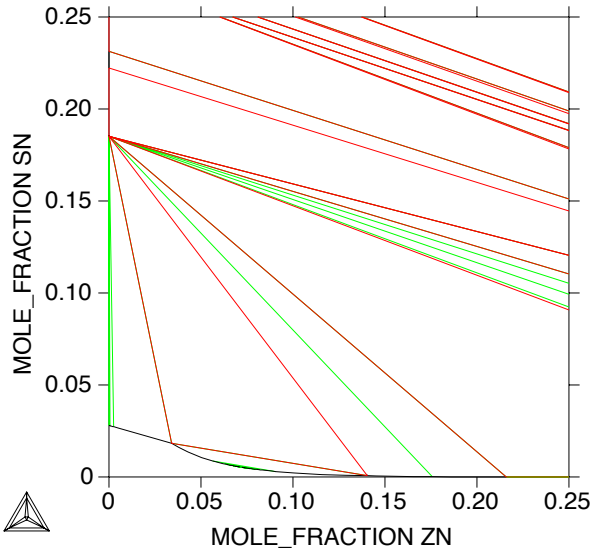

Figure 7. Predicted isothermal sections at various temperatures of the ternary Li-Sn-Zn alloy phase diagram at high Li-content. Besides multi-phase fields, the region of stability of the liquid phase is located in the lower left corner of the isothermal sections. Note that the tie-lines are indicated in green. The phase regions for the isothermal sections at 973 and 673 K are clearly indicated in Figs. 8 and 9.

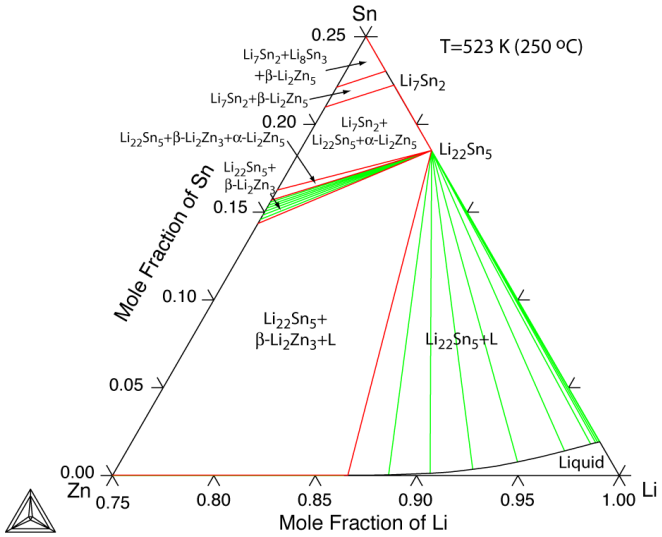
T=523 K (250 ºC)
Sn
Li7Sn2+Li8Sn3
+β-Li2Zn5
Li7Sn2+β-Li2Zn5
Li7Sn2
Li7Sn2+
Li22Sn5+β-Li2Zn5
Li22Sn5+β-Li2Zn3+α-Li2Zn5
Li22Sn5
Li22Sn5+
β-Li2Zn3
Li22Sn5+
β-Li2Zn3+L
Li22Sn5+L
Liquid
Mole Fraction of Sn
Mole Fraction of Li
Zn
Li
0.25
0.20
0.15
0.10
0.05
0.00
0.75
0.80
0.85
0.90
0.95
1.00

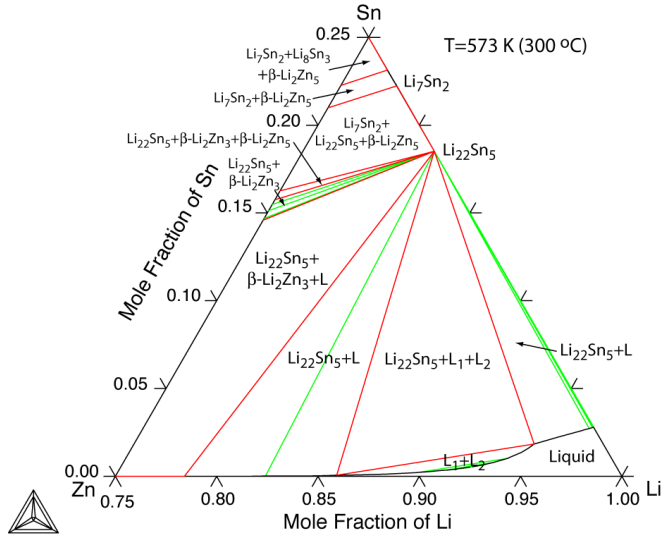
T=573 K (300 ºC)
Sn
Li7Sn2+Li8Sn3
+β-Li2Zn5
Li7Sn2+β-Li2Zn5
Li7Sn2
Li7Sn2+
Li22Sn5+β-Li2Zn5
Li22Sn5+β-Li2Zn3+β-Li2Zn5
Li22Sn5
Li22Sn5+
β-Li2Zn3
Li22Sn5+
β-Li2Zn3+L
Li22Sn5+L
Li22Sn5+L1+L2
L1+L2
Liquid
Mole Fraction of Sn
Mole Fraction of Li
Zn
Li
0.25
0.20
0.15
0.10
0.05
0.00
0.75
0.80
0.85
0.90
0.95
1.00

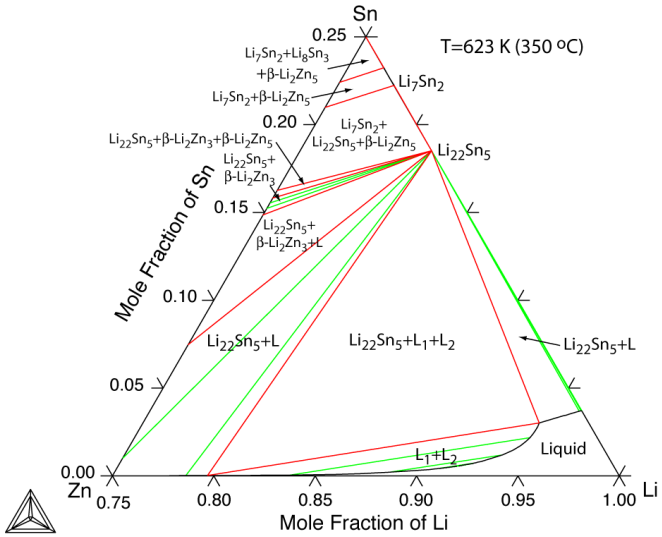
T=623 K (350 ºC)
Sn
Li7Sn2+Li8Sn3
+β-Li2Zn5
Li7Sn2+β-Li2Zn5
Li7Sn2
Li7Sn2+
Li22Sn5+β-Li2Zn5
Li22Sn5+β-Li2Zn3+β-Li2Zn5
Li22Sn5
Li22Sn5+
β-Li2Zn3
Li22Sn5+
β-Li2Zn3+L
Li22Sn5+L
Li22Sn5+L1+L2
L1+L2
Liquid
Mole Fraction of Sn
Mole Fraction of Li
Zn
Li
0.25
0.20
0.15
0.10
0.05
0.00
0.75
0.80
0.85
0.90
0.95
1.00

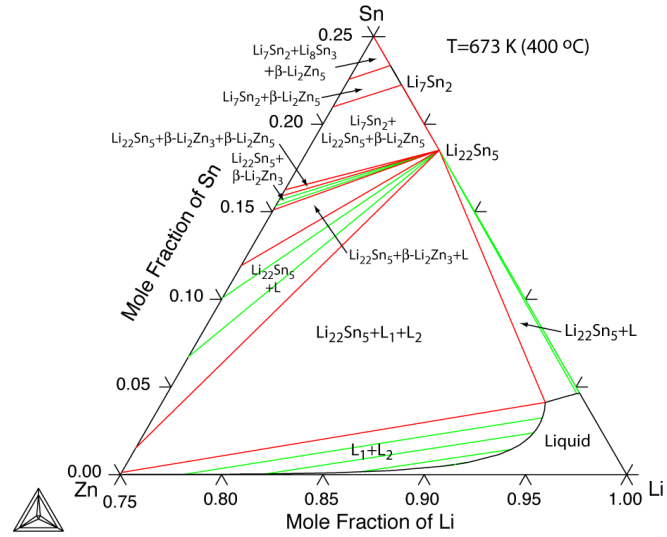
T=673 K (400 ºC)
Sn
Li7Sn2+Li8Sn3
+β-Li2Zn5
Li7Sn2+β-Li2Zn5
Li7Sn2
Li7Sn2+
Li22Sn5+β-Li2Zn5
Li22Sn5+β-Li2Zn3+β-Li2Zn5
Li22Sn5
Li22Sn5+
β-Li2Zn3
Li22Sn5+β-Li2Zn3+L
Li22Sn5
+L
Li22Sn5+L1+L2
Li22Sn5+L
L1+L2
Liquid
Mole Fraction of Sn
Mole Fraction of Li
Zn
Li
0.25
0.20
0.15
0.10
0.05
0.00
0.75
0.80
0.85
0.90
0.95
1.00

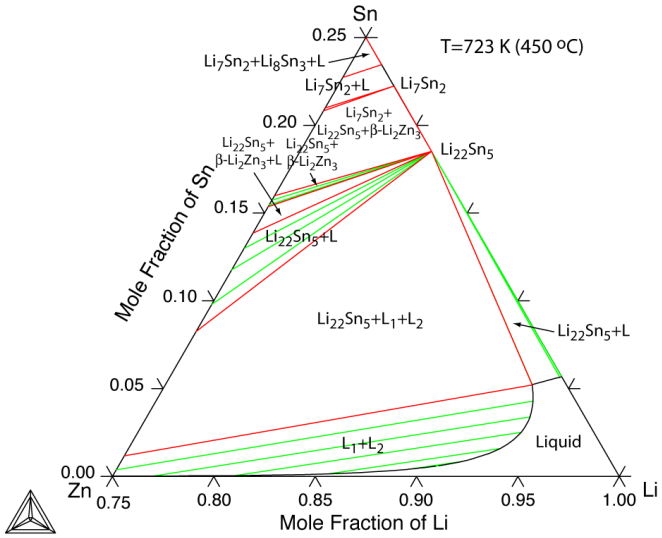
T=723 K (450 ºC)
Sn
Li7Sn2+Li8Sn3+L
Li7Sn2+L
Li7Sn2
Li7Sn2+
Li22Sn5+β-Li2Zn3
Li22Sn5+
β-Li2Zn3+L
Li22Sn5+
β-Li2Zn3
Li22Sn5
Li22Sn5+L
Li22Sn5+L1+L2
Li22Sn5+L
L1+L2
Liquid
Mole Fraction of Sn
Mole Fraction of Li
Zn
Li
0.25
0.20
0.15
0.10
0.05
0.00
0.75
0.80
0.85
0.90
0.95
1.00

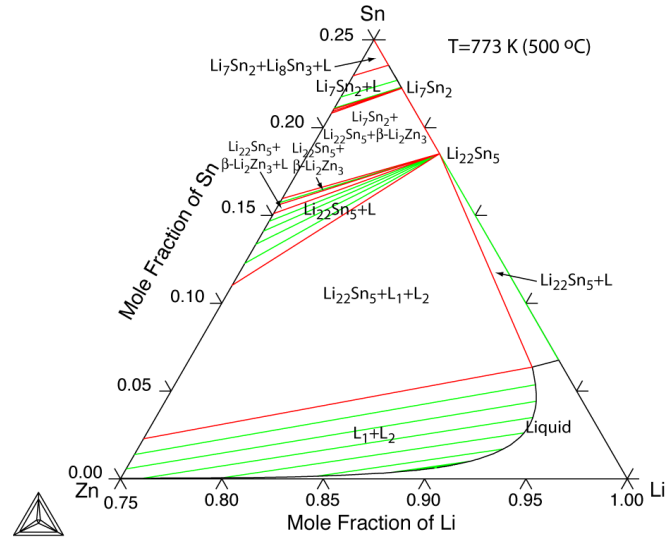
T=773 K (500 ºC)
Sn
Li7Sn2+Li8Sn3+L
Li7Sn2+L
Li7Sn2
Li7Sn2+
Li22Sn5+β-Li2Zn3
Li22Sn5+
β-Li2Zn3+L
Li22Sn5+
β-Li2Zn3
Li22Sn5
Li22Sn5+L
Li22Sn5+L1+L2
Li22Sn5+L
L1+L2
Liquid
Mole Fraction of Sn
Mole Fraction of Li
Zn
Li
0.25
0.20
0.15
0.10
0.05
0.00
0.75
0.80
0.85
0.90
0.95
1.00

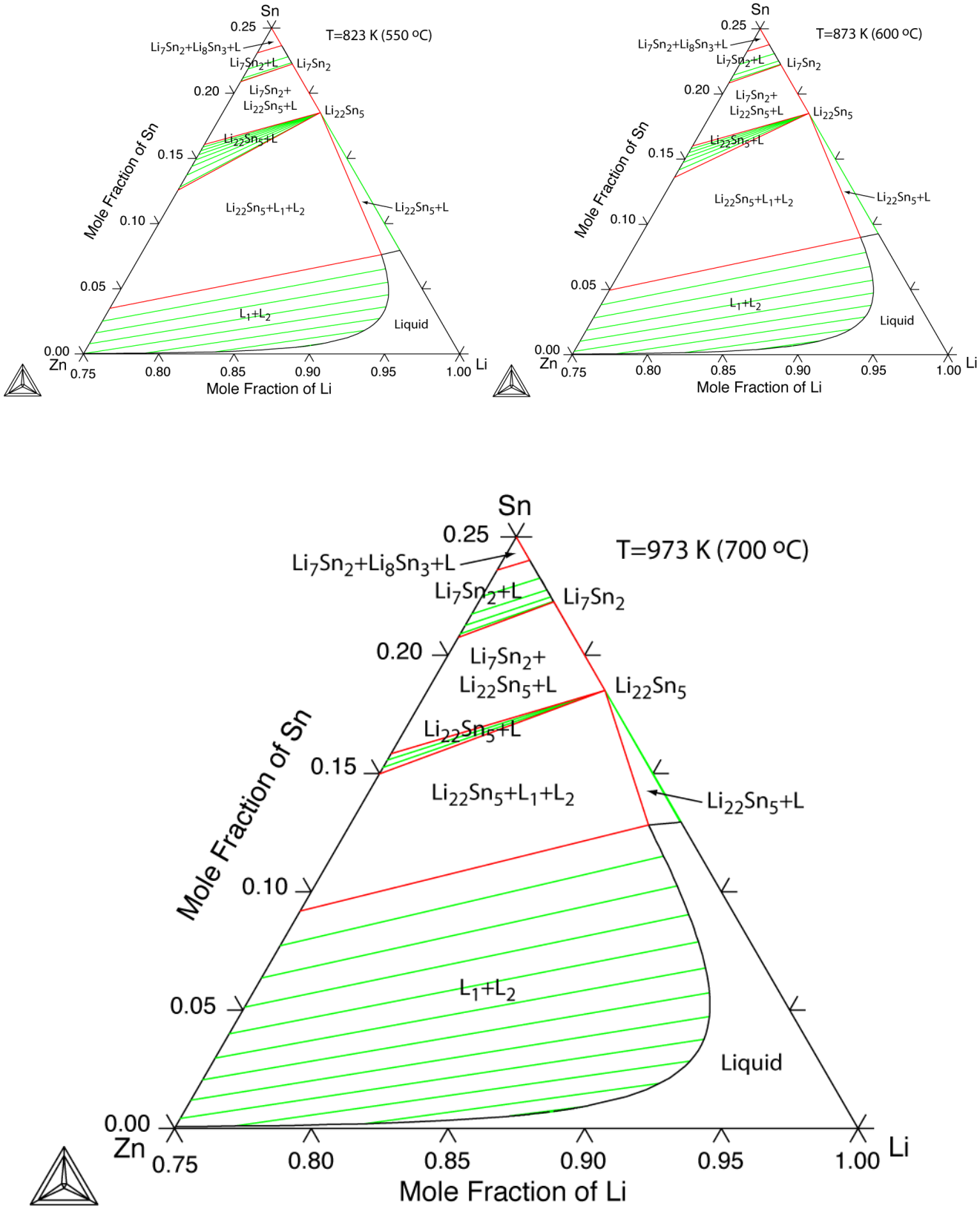

Figure 8. High Li-content portions of the predicted isothermal sections of the ternary Li-Sn-Zn alloy phase diagram from 523 K to 973 K. Besides multi-phase fields, the region of stability of the liquid phase is located in the lower left corner of the isothermal sections. Note that the tie-lines are indicated in green.

Two typical isothermal sections of the Li-Sn-Zn phase diagram are shown in Fig. 9 at 973 K (700 ºC) and 673 K (400 ºC).

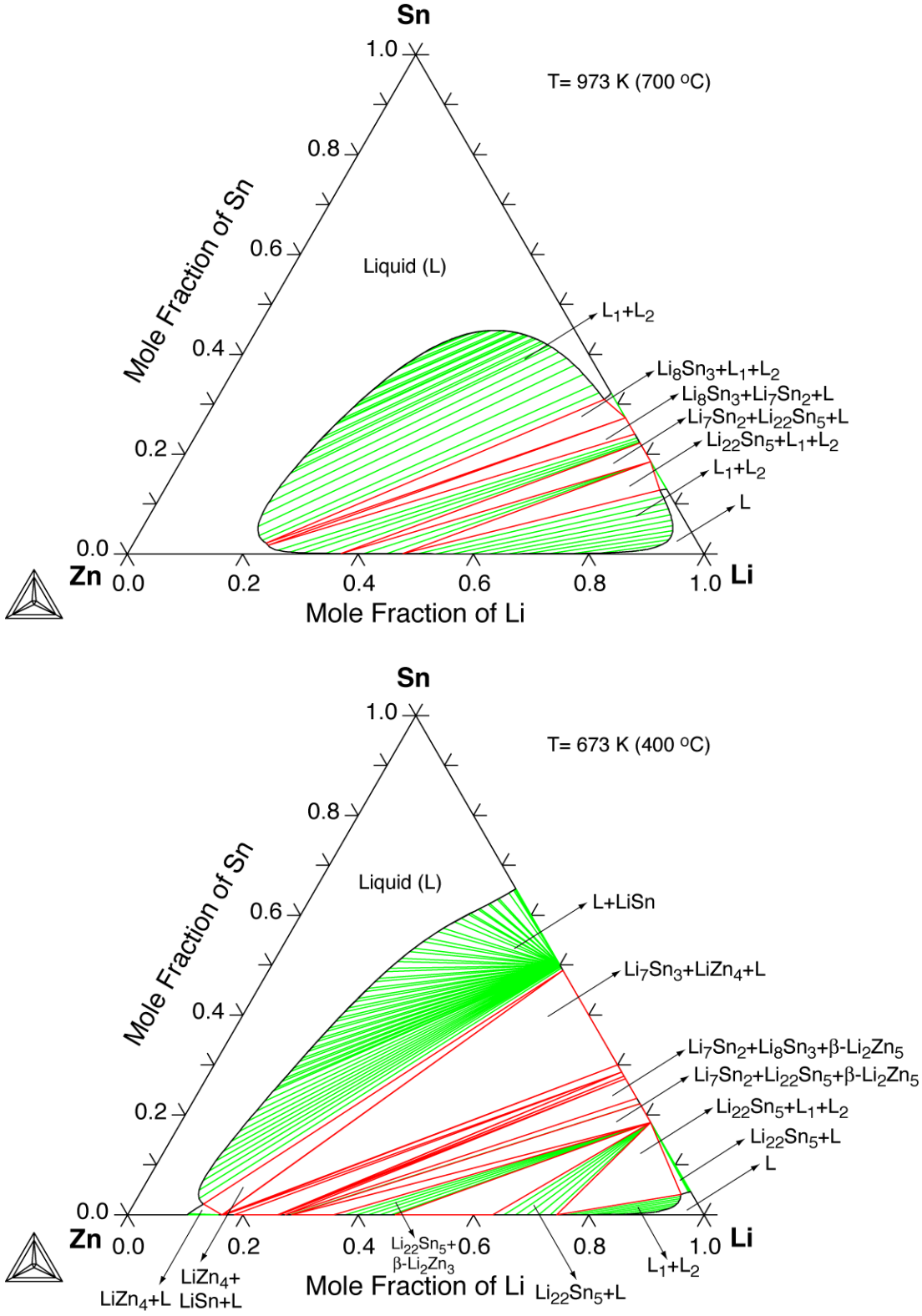

Figure 9. Predicted isothermal sections of the ternary Li-Sn-Zn alloy system at 973 K (700 ºC) and 673 K (400 ºC).

The isothermal sections of the ternary Li-Sn-Zn presented in Fig. 7 lead to the definition of the liquidus surface at high Li-content shown in Fig. 10 below, with the liquid state located on the left side of the figure. It worth noting in Fig. 8 the existence of a two-phase region indicating two immiscible liquids (L_1 and L_2) that, for the current purpose, extends the domain of stability of the liquid phase.

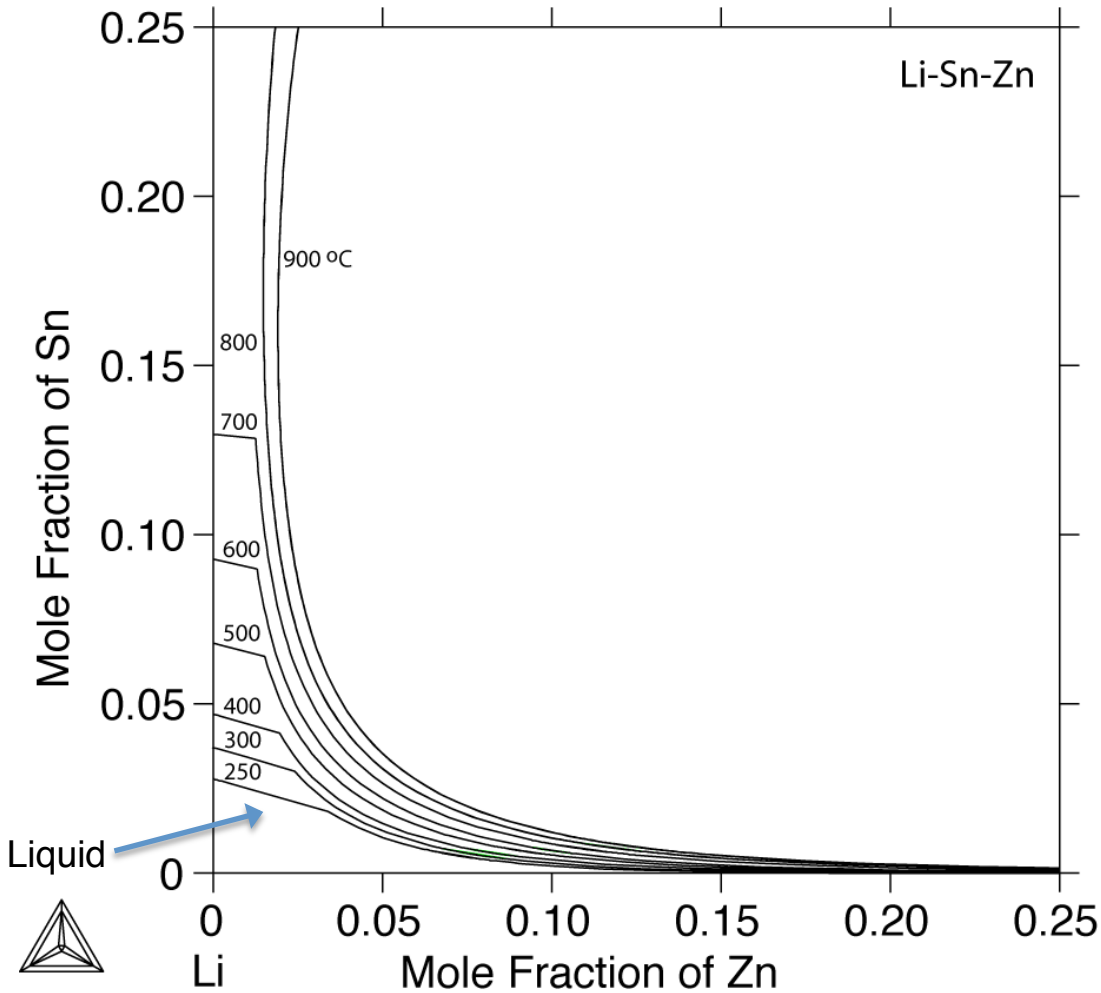

Figure 10. Predicted liquidus surface at high Li-content for the ternary Li-Sn-Zn alloy system. The liquidus surface is defined from the isothermal lines from 900 to 300 ºC, plus an additional line associated with the low temperature of 250 ºC.

Conclusions

The thermodynamic properties of the three binaries Li-Sn, Li-Zn, and Sn-Zn alloy systems have been generated, and isothermal sections of the ternary Li-Sn-Zn phase diagram have been proposed. Because of the lack of experimental results on calorimetric data (energetics) and phase characterization, further validation is required, and these data will provide an opportunity to revise and further validate the thermodynamic data for the Li-based alloys.

In summary, for the first semester the accomplishments are:

1. Extensive literature search on phase stability properties of the three subsystems that make up the ternary Li-Sn-Zn alloy system alloys has been completed.
2. Within the CALPHAD framework, the three binary phase diagrams (Li-Sn, Li-Zn, and Sn-Zn) have been assessed with a input data from previous assessments.
3. The thermodynamic data for the three binaries have been put together to study the thermodynamic properties and the phase diagram of the ternary Li-Sn-Zn alloy system.
4. Based on the current thermodynamic description of the ternary Li-Sn-Zn system, that would need to be experimentally validated, the liquid state extends in a narrow region of solutes Sn and Zn near pure Li.
5. Besides Sn and Zn, other elements, as indicated in Appendix D, could be considered, based solely on how they chemically interact with Li, and the thermodynamic properties of the mixtures. However detailed neutronic calculations are required before making any decision on their selection.

Acknowledgments

This work was performed under the auspices of the U.S. DOE by LLNL under Contract DE-AC52-07NA27344 and funded by the Laboratory Directed Research and Development Program at LLNL under project tracking code 14-ER-035.

References

[1] ASM Alloy Phase Diagrams Center, P. Villars, editor-in-chief; H. Okamoto and K. Cenzual, section editors; http://www1.asminternational.org/AsmEnterprise/APD, ASM International, Materials Park, OH, 2006.

[2] J. Sangster, and C. W. Bale, The Li-Sn (Lithium-Tin) System, J. Phase Equilib. **19**, 70-75 (1998).

Y. Liang, Z. Du, C. Guo, and C., "Thermodynamic modeling of the Li-Zn system, J. Alloys Compd. **455**, 236-242 (2008).

[4] K. Doi, S. Ono, H. Ohtani, and M. Hasebe, "Thermodynamic Study of the Phase Equilibria in the Sn-Ti-Zn Ternary System", J. Phase Equilib. Diffus. **27**, 63-74 (2006).

[5] Z. Du, Z. Jiang, and C. Guo, "Thermodynamic optimizing of the Li-Sn system", Z. Metallkd. **97**, 10-16 (2006).

[6] D. Henriques, V. Motalov, L. Bencze, S. Fürtauer, and T. Markus, "Experimental thermodynamics of the Li-Sn system by Knudsen Effusion Mass Spectrometry", J. of Alloys and

Compounds **585**, 299-306 (2014).

[7] Yu Liang, Zhenmin Du, Cuiping Guo, and Changrong Li, "Thermodynamic Modeling of the Li-Zn System", J. of Alloys and Compounds **455**, 236-242 (2008).

[8] Cuiping Guo, Yu Liang, Changrong Li, and Zhenmin Du, "Thermodynamic description of the Al–Li–Zn system", CALPHAD **35**, 54-65 (2011).

[9] H. Ohtani, M. Miyashita, and K. Ishida, "Thermodynamic study of phase equilibria in the Sn-Ag-Zn system", J. Jpn. Inst. Metals **63** (6), 685-694 (1999).

[10] Y. Cui, X.J. Liu, I. Ohnuma, R. Kainuma, and H. Ohtani, K. Ishida, "Thermodynamic calculation of the In–Sn–Zn ternary system", J. of Alloys and Compounds **320**, 234-241 (2001).

[11] Jiri Vizdal, Maria Helena Braga, Ales Kroupa, Klaus W. Richter, Delfim Soares, Luís Filipe Malheiros, and Jorge Ferreira, "Thermodynamic assessment of the Bi–Sn–Zn System", CALPHAD **31**, 438-448 (2007).

[12] Ching-feng Yang, Feng-ling Chen,Wojciech Gierlotka, Sinn-wen Chen, Ker-chang Hsieh, and Li-ling Huang, "Thermodynamic properties and phase equilibria of Sn–Bi–Zn ternary alloys", Mater. Chem. and Phys. **112**, 94-103 (2008).

[13] Yu-chih Huang, Sinn-wen Chen, Chin-yi Chou, and Wojciech Gierlotka, "Liquidus projection and thermodynamic modeling of Sn–Zn–Cu ternary system", J. of Alloys and Compounds **477**, 283-290 (2009).

[14] G. Vassilev, V. Gandova, N. Milcheva, and G. Wnuk, "Thermodynamic description of the system Ag-Sn-Zn", CALPHAD **43**, 133-138 (2013)

[15] Y. M. Muggianu, M. Gambino, and J. P. Bros, "Enthalpies de Formation des Alliages Liquides Bismuth-Etain-Gallium à 723 K. Choix d'une Représentation Analytique des Grandeurs d'Excès Intégrales et Partielles de Mélange", J. Chem. Phys. **22**, 83-88 (1975).

Appendix A. Thermo-Calc Application Software and CALPHAD Modeling

Thermo-Calc version S [A1] is a commercially available software code that fulfills the need for critical modeling and analysis of data to:

• Produce, refine, and analyze multi-component phase diagrams of alloys at relevant temperatures for predicting phase stability properties.

• Determine the solidification path and long-term aging of alloys.

• Generate isothermal sections of multi-component alloy phase diagrams at relevant temperatures, isopleths, and property diagrams (phase fractions as functions of temperature), and composition versus temperature for all stable and metastable phases forming.

• Simulate phase transformations according to the Scheil-Gulliver model (for which local equilibria, infinite diffusion in the liquid phase, and no back diffusion in the solid phase are assumed).

Thermo-Calc is specially designed for systems with strongly non-ideal phases. It has gained a worldwide reputation as the best software application for calculation of multi-component phase diagrams. It is the only commercially available software that can calculate arbitrary phase diagram sections with up to five independent variables in multi-component systems. There are also modules to calculate many other types of properties, such as, Scheil-Gulliver solidification simulations, Pourbaix diagrams, partial pressures in gases, and more [A1].

In the CALPHAD approach [A2-A7], the Gibbs energy of individual phases is modeled, and the model parameters are collected in a thermodynamic database. It is the modeling of the Gibbs energy of individual phases and the coupling of phase diagram and thermo-chemistry that make the CALPHAD a powerful technique in computational thermodynamics of multi-component materials. Models for the Gibbs energy are based on the crystal structures of the phases. For pure elements and stoichiometric compounds, the most commonly used model is the one suggested by the Scientific Group Thermodata Europe (SGTE) [A8] and has the following form (for simplicity, the pressure dependence and the magnetic contribution are not shown here),

$$G_m - H_m^{SER} = a + bT + cT\ln(T) + \sum d_i T^i \qquad \text{(A.1)}$$

The left-hand side of Eq. A.1 is defined as the Gibbs energy relative to a standard element reference state (SER), where H_m^{SER} is the enthalpy of the element in its stable state at 298.15 K and 1 bar of pressure. Coefficients, a, b, c, and d_i are the model parameters. The SGTE data for all the pure elements of the periodic table have been compiled by Dinsdale [A8].

For multi-component solution phases, the Gibbs energy has the following general expression [A2,A3,A6A7],

$$G = G^o + G_{mix}^{ideal} + G_{mix}^{xs} \tag{A.2}$$

where G^o is the contribution from the mechanical mixing of the pure components, G_{mix}^{ideal} is the ideal mixing contribution, and G_{mix}^{xs} is the excess Gibbs energy of mixing due to non-ideal interactions. Sublattice models have been widely used to describe solution phases [A3, A6, A7]. For example, for a simple phase with two sublattices in an A-B binary system where the two components enter both sublattices, the sublattice model is written as $(A,B)_p(A,B)_q$, where subscripts p and q denote the number of sites of each sublattice. More specifically, the three terms in Eq. A.2 are written as,

$$G^o = y_A^I y_A^{II} G_{A:A}^o + y_A^I y_B^{II} G_{A:B}^o + y_B^I y_A^{II} G_{B:A}^o + y_B^I y_B^{II} G_{B:B}^o \tag{A.3}$$

$$G_{mix}^{ideal} = pRT\left(y_A^I \ln y_A^I + y_B^I \ln y_B^I\right) + qRT\left(y_A^{II} \ln y_A^{II} + y_B^{II} \ln y_B^{II}\right) \tag{A.4}$$

$$\begin{aligned} G_{mix}^{xs} = {} & y_A^I y_B^I \left(y_A^{II} \sum_{k=0} L_{A,B:A}^k (y_A^I - y_B^I)^k + y_B^{II} \sum_{k=0} L_{A,B:B}^k (y_A^I - y_B^I)^k \right) \\ & + y_A^{II} y_B^{II} \left(y_A^I \sum_{k=0} L_{A:A,B}^k (y_A^{II} - y_B^{II})^k + y_B^I \sum_{k=0} L_{B:A,B}^k (y_A^{II} - y_B^{II})^k \right) \end{aligned} \tag{A.5}$$

where y^I and y^{II} are the site fractions of A or B in the first and second sublattices, respectively. $G_{I:J}^o$ is the Gibbs energy of the compound I_pJ_q, expressed by Eq. 1. $L_{A,B:*}^k$ ($L_{*:A,B}^k$) is the kth order interaction parameter between component A and B in the first (second) sublattice. In this notation, a colon separates components occupying different sublattices, and a comma separates interacting components in the same sublattice. These equations can be generalized for phases with multi-components and multi-sublattices, and they reduce to a random substitutional model when there is only one sublattice.

For a multi-component solution in a particular phase Φ described with a single sublattice model, the three contributions to the total Gibbs energy reduce to [A3, A6, A7]:

$$\begin{aligned} {}^{\Phi}G^o &= \sum_I c_I \, {}^{\Phi}G_I^o \\ {}^{\Phi}G_{mix}^{ideal} &= RT \sum_I c_I \ln c_I \\ {}^{\Phi}G_{mix}^{xs} &= \sum_I \sum_{J>I} c_I c_J \sum_k {}^{\Phi}L_{I,J}^k \left(c_I - c_J\right)^k \end{aligned} \tag{A.6}$$

where the molar Gibbs energy of mixing is expressed by a Redlich-Kister expansion [A9]. In these expressions c_I is the composition of the alloy in species I, and the $L_{I,J}^k$ is the kth-order binary interaction parameter between species I and J usually expressed as a first-order polynomial in temperature T: $L_{I,J}^k = a_{I,J}^k + b_{I,J}^k T$. Note that in both sets of expressions the excess

Gibbs energy due to non-ideal contributions is expressed within the Muggianu approximation [A10].

It is worth mentioning that data generated with the Thermo-Calc software also provide the basis for more accurate predictions of diffusion kinetics and ultimately TTT (temperature-time-transformations) diagrams with the DICTRA software [A1, A11] by assuming diffusion both in the liquid and the solid phase. Note that the results of both equilibrium solidification and Scheil-Gulliver simulations generated by Thermo-Calc correspond to upper and lower bounds for the DICTRA results.

Input data files used by Thermo-Calc are: KP (Kaufman binary alloys database), SSOL5 (Scientific Group Thermodata Europe, or SGTE, solution database), from published journals, and/or from qualified sources. Here to describe the selected alloys systems, a thermodynamic database has been developed.

References

A1. The Thermo-Calc and DICTRA applications software are products of Thermo-Calc AB; B. Sundman, B. Jansson, and J.-O. Andersson, "The Thermo-Calc Databank System", CALPHAD **9** (4), 153 (1985); J.-O. Andersson, T. Helander, L. Höglund, Pingfang Shi, and B. Sundman, "THERMO-CALC & DICTRA, computational tools for materials science", CALPHAD **26** (2), 273-312 (2002); cf. also http://www.thermocalc.se.

A2. L. Kaufman and H. Bernstein, "*Computer Calculation of Phase Diagrams with Special Reference to Refractory Metals*" (Academic Press, New York, 1970).

A3. N. Saunders and A. P. Miodownik, "*CALPHAD, Calculation of Phase Diagrams: A Comprehensive Guide*", Pergamon Materials Series, vol. 1, ed. by R W. Cahn (Pergamon Press, Oxford, 1998).

A4. A. P. Miodownik, "Phenomenological calculations of phase equilibria: the CALPHAD approach", in NATO-ASI Proceedings, Series B: Physics, Vol. **319**, eds. P. E. A. Turchi and A. Gonis (Plenum Press, NY, 1994), p. 45-79.

A5. MRS Bulletin, Vol. **24**, No. 4 (April 1999), "*Computer Simulations from Thermodynamic Data: Materials Production and Development*", p. 18-49.

A6. "*CALPHAD and Alloy Thermodynamics*", ed. by P. E. A. Turchi, A. Gonis, and R. D. Shull (TMS Publication, Warrendale, PA, 2002); and references therein.

A7. Hans Leo Lucas, Suzana G. Fries, and Bo Sundman, "*Computational Thermodynamics – The Calphad Method*" (Cambridge University Press, Cambridge, 2007).

A8. A. Dinsdale, "SGTE Database for Pure Elements", CALPHAD **15**, 317-425 (1991).

A9. O. Redlich and A. Kister, "Algebraic Representation of the Thermodynamic Properties and the Classification of Solutions", Ind. Eng. Chem. **40**, 345-348 (1948).

A10. Y. M. Muggianu, M. Gambino, and J. P. Bros, "Enthalpies de Formation des Alliages Liquides Bismuth-Etain-Gallium à 723 K. Choix d'une Représentation Analytique des Grandeurs d'Excès Intégrales et Partielles de Mélange", J. Chem. Phys. **22**, 83-88 (1975).

A11. A. Engström, L. Höglund, and J. Ågren, "Computer simulations of diffusion in multiphase systems", Metall. Mater. Trans. **25A**, 1127-1134 (1994); A. Borgenstam, A. Engström, L. Höglund, and J. Ågren, "DICTRA, a tool for simulation of diffusional transformations in alloys", J. of Phase Equil. **21** (3), 269-280 (2000).

Appendix B. Thermodynamic database "LSF_F.TDB" for Li-Sn, Li-Zn, and Sn-Zn

The following TDB file is used in conjunction with the Thermo-Calc software [B1] to calculate equilibrium phase diagrams and other thermodynamic properties.

The data for the pure elements are obtained from the SGTE database (SSOL5) as reported by Dinsdale [B2]. For the gas phase, the data have been collected for the PURE4 database

First the thermodynamic data are given in accordance with the formalism described in Appendix A. Then follows the description of the thermodynamic data file (LSZ_F.TDB) as used by the Thermo-Calc software.

********** **Li-Sn** **********

Zhenmin Du, Zhenquan Jiang, and Cuiping Guo, "Thermodynamic optimizing of the Li-Sn system", Z. für Metallkd. **97**, 10-16 (2006).

Liquid – Model **(**Li**,**Sn**)**$_1$
L(LIQUID,LI,SN;0) -121142.2+24.0000*T
L(LIQUID,LI,SN;1) -87650.9+24.0000*T
L(LIQUID,LI,SN;2) -11383.3-8.7985*T
L(LIQUID,LI,SN;3) +37847.8-37.6298*T

bcc_A2 – Model **(**Li**,**Sn**)**$_1$
G(BCC_A2, SN:VA;0)) +4400.0-6.0000*T+GHSERSN 100.0–3000.0 K
L(BCC_A2,LI,SN;VA;0) -92821.4-19.3685*T
L(BCC_A2,LI,SN:VA;1) -79522.7

Diamond_A4 – Model **(**Sn**)**$_1$**(**VA**)**$_1$
G(DIAMOND_A4,SN:VA) -9579.608+114.007785*T-22.972*T*LN(T)-
0.00813975*T**2+2.7288E-06*T**3+25615*T**(-1) 100.00–298.15 K
G(DIAMOND_A4,SN:VA) -9063.001+104.84654*T-21.5750771*T*LN(T)-
0.008575282*T**2+1.784447E-06*T**3+25615*T**(-1) 298.15–800.00 K
G(DIAMOND_A4,SN:VA) -10909.351+147.396535*T-28.4512*T*LN(T) 800.00–3000.00 K

$Li_{22}Sn_5$ – Model (Li)$_{22}$**(**Sn**)**$_5$
G(LI22SN5,LI:SN;0) -1095242.7+270.00*T+22*GHSERLI+5*GHSERSN

Li_7Sn_2 – Model (Li,Sn)$_7$**(**Sn**)**$_2$
G(LI7SN2,LI:SN;0) -383551.0+81.00*T+7*GHSERLI+2*GHSERSN
G(LI7SN2,SN:SN;0) +27000.0 +9*GHSERSN
G(LI7SN2,LI,SN:SN;0) +979887.1+9.0115*T
G(LI7SN2,LI,SN:SN;1) -1457538.4+27.5363*T

Li_8Sn_3 – Model (Li)$_8$**(**Sn**)**$_3$
G(LI8SN3,LI:SN;0) -477620.1+90.00*T+8*GHSERLI+3*GHSERSN

$Li_{13}Sn_5$ – Model (Li)$_{13}$**(**Sn**)**$_5$

G(LI3SN5,LI:SN;0) -780902.1+145.00*T+13*GHSERLI+5*GHSERSN

Li_5Sn_2 – Model $(Li)_5(Sn)_2$
G(LI5SN2,LI:SN;0) -302420.0+54.00*T+5*GHSERLI+2*GHSERSN

Li_7Sn_3 – Model $(Li)_7(Sn)_3$
G(LI7SN3,LI:SN;0) -428079.0+75.00*T+7*GHSERLI+3*GHSERSN

LiSn – Model $(Li)_1(Li,Sn)_{\backslash 1}$
G(LISN,LI:SN;0) -73198.3+9.85*T+GHSERLI+GHSERSN
G(LISN,LI:LI;0) +6000.00+2*GHSERLI
G(LISN,LI:LI,SN;0) -45169.2
G(LISN,LI:LI,SN;1) +34205.5

Li_2Sn_5 – Model $(Li)_2(Sn)_5$
G(LI2SN5,LI:SN;0) = -196683.0+90.00*T+2*GHSERLI+5*GHSERSN

********** **Li-Zn** **********

Cuiping Guo, Yu Liang, Changrong Li, and Zhenmin Du, "Thermodynamic description of the Al–Li–Zn system", CALPHAD **35**, 54-65 (2011). N. B.: the three binaries are described in other papers: Al-Li in Hallstedt *et al*. (2007), Al-Zn in Mathon *et al.* (2000), and Li-Zn in Liang *et al*. (2008).

Liquid – Model $(Li,Zn)_1$
L(LIQUID,LI,ZN;0) -45258.6+26.3677*T
L(LIQUID,LI,ZN;1) +22887.2-4.1921*T
L(LIQUID,LI,ZN;2) -4552.6+4.0715*T

fcc_A1 – Model $(Li,Zn)_1$
G(FCC_A1,LI;0) = -108+1.3*T+GHSERLI 200.0–3000.0 K
G(FCC_A1,ZN;0) = +2969.82-1.56968T+GHSERZN 298.15–1700.0 K

bcc_A2 – Model $(Li,Zn)_1$
G(BCC_A2, ZN;0) = +2886.96-2.5104*T+GHSERZN 298.15–1700.0 K
L(BCC_A2,LI,ZN:VA;0) -54260.4+45.7720*T
L(BCC_A2,LI,ZN:VA;2) +25153.3

hcp_A3 – Model $(Li,Zn)_1$
G(HCP_A3,LI;0) = -154+2*T+GHSERLI 200.0–3000.0 K
G(HCP_A3,ZN;0) = +GHSERZN 298.15–1700.0 K
L(HCP_A3,LI,ZN:VA;0) -29301.5−0.2586*T
L(HCP_A3,LI,ZN:VA;1) +15702.2+3.5167*T

B32 – Model $(Li,Zn)_{0.5}(Li,Zn)_{0.5}$
G(B32,LI:ZN;0) = G(B32,ZN:LI;0) = −26930.7+10.0062*T
L(B32,LI,ZN:LI;0) = L(B32,LI:LI,ZN;0) = -26474.4+30.2611*T
L(B32,LI,ZN:LI;1) = L(B32,LI:LI,ZN;1) = -11635.9+1.4065*T
L(B32,LI,ZN:ZN;0) = L(B32,ZN:LI,ZN;0) = -13623.4+1.7890*T
L(B32,LI,ZN:ZN;1) = L(B32,ZN:LI,ZN;1) = -4786.0-4.0231*T

β Li_2Zn_3 – Model $(Li,Zn)_2(Li,Zn)_3$
G(Li2Zn3_B,LI:ZN;0) = +2*GHSERLI+3*GHSERZN-84218.4+27.7580*T
G(Li2Zn3_B,ZN:LI;0) = +2*GHSERZN+3*GHSERLI+84218.4-27.7580*T
G(Li2Zn3_B,LI:LI;0) = +5*GHSERLI+9307.8
G(Li2Zn3_B,ZN:ZN;0) = +5*GHSERZN+9307.8
L(Li2Zn3_B,LI,ZN:LI;0) = L(Li2Zn3_B,LI,ZN:ZN;0) = -87667.3+59.7976*T
L(Li2Zn3_B,LI,ZN:LI;1) = L(Li2Zn3_B,LI,ZN:ZN;1) = +49513.8-70.0108*T
L(Li2Zn3_B,LI:LI,ZN;0) = L(Li2Zn3_B,ZN:LI,ZN;0) = +7367.6+6.9984*T
L(Li2Zn3_B,LI:LI,ZN;1) = L(Li2Zn3_B,ZN:LI,ZN;1) = +8734.9-11.9000*T

α Li_2Zn_3 – Model $Li_2(Li,Zn)_3$
G(Li2Zn3_A,LI:ZN;0) = +2*GHSERLI+3*GHSERZN-85329.5+30.2362*T
G(Li2Zn3_A,LI:LI;0) = +5*GHSERLI+19964.61
L(Li2Zn3_A,LI:LI,ZN;0) = -7720.6+12.5469*T
L(Li2Zn3_A,LI:LI,ZN;1) = +1001.2+1.0073*T

β Li_2Zn_5 – Model $(Li,Zn)_2(Zn)_5$
G(Li2Zn5_B,LI:ZN;0) = +2*GHSERLI+5*GHSERZN-122836.0+51.4932*T
G(Li2Zn5_B,ZN:ZN;0) = +7*GHSERZN+26766.0
L(Li2Zn5_B,LI,ZN:ZN;0) = -13440.5
L(Li2Zn5_B,LI,ZN:ZN;1) = -21665.2

α Li_2Zn_5 – Model $(Li,Zn)_2(Zn)_5$
G(Li2Zn5_A,LI:ZN;0) = +2*GHSERLI+5*GHSERZN-123038.9+51.8671*T
G(Li2Zn5_A,ZN:ZN;0) = +7*GHSERZN+12169.3
L(Li2Zn5_A,LI,ZN:ZN;0) = -12463.9

$LiZn_2$ – Model $Li(Zn)_2$
G(LiZn2,LI:ZN;0) = +GHSERLI+2*GHSERZN-53133.9+23.4266*T

β $LiZn_4$ – Model $(Li,Zn)_{0.2}(Li,Zn)_{0.8}$
G(LiZn4_B,LI:ZN;0) = -191.117297-0.0855*T
G(LiZn4_B,ZN:LI;0) = +191.117297+0.0855*T
L(LiZn4_B,LI:LI,ZN;0) = +20574.6225-7.4146*T
L(LiZn4_B,ZN:LI,ZN;0) = +19682.1-7.8141*T
L(LiZn4_B,LI:LI,ZN;1) = 1LβLiZn4.Zn:Li,Zn = -29447.8+33.0299*T
L(LiZn4_B,LI,ZN:LI;0) = +4904.8-1.9606*T
L(LiZn4_B,LI,ZN:ZN;0) = +5159.5-1.8466*T
L(LiZn4_B,LI,ZN:LI;1) = 1LβLiZn4.Li,Zn:Zn = -7361.9+8.2575*T

α $LiZn_4$ – Model $(Li,Zn)(Li,Zn)_4$
G(LiZn4_A,LI:ZN;0) = +GHSERLI+4*GHSERZN-78372.0+43.2115*T
G(LiZn4_A,ZN:LI;0) = +GHSERZN+4*GHSERLI+78372.0-43.2115*T
G(LiZn4_A,LI:LI;0) = +5*GHSERLI+15000.0
G(LiZn4_A,ZN:ZN;0) = +5*GHSERZN+15000.0
L(LiZn4_A,LI,ZN:LI;0) = L(LiZn4_A,LI,ZN:ZN;0) = -33953.6+20.1515*T
L(LiZn4_A,LI:LI,ZN;0) = L(LiZn4_A,ZN:LI,ZN;0) = -18698.3+7.7695*T

********** **Sn-Zn** **********

Yu-chih Huang, Sinn-wen Chen, Chin-yi Chou, and Wojciech Gierlotka, "Liquidus projection and thermodynamic modeling of Sn–Zn–Cu ternary system", J. of Alloys and Compounds **477**, 283-290 (2009).

Liquid
L(LIQUID,SN,ZN;0) +21360.454-97.1651*T+11.4877*T*LN(T)
L(LIQUID,SN,ZN;1) -5137.954-0.1805*T+0.5199*T*LN(T)
L(LIQUID,SN,ZN;2) +1716.54532

fcc_A1
L(FCC_A1,SN,ZN:VA;0) +59658.680

bcc_A2
L(BCC_A2,SN,ZN:VA;0) +12000

bct_A5
L(BCT_A5,SN,ZN;0) +6846.010+24.5560*T

hcp_Zn
L(HCP_ZN,SN,ZN:VA;0) +21310.7476+65.5652*T

****

Then follows the description of the thermodynamic data file (LSZ_F.TDB) as used by the Thermo-Calc software.

```
$ Database File *** LSZ_F.TDB *** written on 11/18/2013
$
$ *** Sn-Zn ***
$ From Ref.10 Y.-C. Huang, S.-W. Chen, C.-Y. Chou, and W. Gierlotka,
$        Liquidus projection and thermodynamic modeling of Sn-Zn-Cu
$        ternary system, J. of Alloys and Compounds 477, 283-290 (2009).
$
$ *** Li-Sn ***
$ From Ref.11 Zhenmin Du, Zhenquan Jiang, and Cuiping Guo, Thermodynamic
$      optimizing of the Li-Sn system, Z. für Metallkd. 97, 10-16 (2006).
$
$ *** Li-Zn ***
$ From Ref.12 C. Guo, Y. Liang, C. Li, and Z. Du, Thermodynamic description
$      of the Al-Li-Zn system, CALPHAD 35, 54-65 (2011).
$
$ Pure Elements from Database: SSOL4
$
 ELEMENT /-   ELECTRON_GAS              0.0000E+00  0.0000E+00  0.0000E+00!
 ELEMENT VA   VACUUM                    0.0000E+00  0.0000E+00  0.0000E+00!
 ELEMENT LI   BCC_A2                    6.9410E+00  4.6233E+03  2.9095E+01!
 ELEMENT SN   BCT_A5                    1.1871E+02  6.3220E+03  5.1195E+01!
 ELEMENT ZN   HCP_A3                    6.5390E+01  5.6568E+03  4.1631E+01!

 SPECIES LI2                          LI2!
 SPECIES SN2                          SN2!

 FUNCTION F12239T    298.15  +152984.64+2.33568506*T-21.07772*T*LN(T)
  +2.515552E-04*T**2-3.41354333E-08*T**3+7690.735*T**(-1); 2400 Y
   +183390.413-110.69493*T-7.20516*T*LN(T)-.002217371*T**2
  +2.443155E-08*T**3-11648370*T**(-1); 4800 Y
```

```
  +109652.446+17.2445126*T-21.24264*T*LN(T)-.0015038825*T**2
 +3.76717667E-08*T**3+50092500*T**(-1); 8800 Y
  -72231.6406+344.035356*T-57.87689*T*LN(T)+.0017448465*T**2
 -1.58650733E-08*T**3+2.178053E+08*T**(-1); 10000 N !
FUNCTION F12319T    298.15  +203319.119+52.2617041*T-37.02637*T*LN(T)
 -8.421915E-04*T**2-1.078653E-07*T**3+65874.15*T**(-1);  1100 Y
  +200885.055+48.6776391*T-35.9057*T*LN(T)-.0039990175*T**2
 +5.08151333E-07*T**3+883657*T**(-1); 1900 Y
  +137315.894+473.019388*T-93.02457*T*LN(T)+.018440525*T**2
 -1.12358533E-06*T**3+13866255*T**(-1); 3100 Y
  +638944.289-1507.74849*T+153.9314*T*LN(T)-.035715045*T**2
 +1.10781833E-06*T**3-1.776338E+08*T**(-1); 5100 Y
  -624845.177+1789.13827*T-234.2722*T*LN(T)+.0173718*T**2
 -2.55232167E-07*T**3+5.95322E+08*T**(-1); 6000 N !
FUNCTION F15456T    298.15  +299805.017-138.265505*T-2.769934*T*LN(T)
    -.025123235*T**2+2.91121E-06*T**3-225080.65*T**(-1);  500 Y
     +299818.158-153.051454*T+.006576569*T*LN(T)-.031759785*T**2
    +5.12529167E-06*T**3-157706.25*T**(-1); 900 Y
     +259620.873+283.605387*T-63.72523*T*LN(T)+.0132323*T**2
    -8.43548E-07*T**3+4603149.5*T**(-1); 2000 Y
     +305551.58+10.5671675*T-27.57385*T*LN(T)+5.86253E-04*T**2
    -1.41879667E-08*T**3-6339225*T**(-1);  6600 Y
     +330332.683-10.457896*T-25.61849*T*LN(T)+7.907715E-04*T**2
    -2.626045E-08*T**3-39037215*T**(-1); 10000 N !
FUNCTION F15470T    298.15  +415023.293-24.2764849*T-36.02127*T*LN(T)
    -.005866135*T**2+7.95920667E-07*T**3-134064.05*T**(-1);  1100 Y
     +418717.2-28.8639596*T-36.06067*T*LN(T)-.003023904*T**2
    +1.82022167E-07*T**3-1196854*T**(-1); 3000 Y
     +318814.516+319.936469*T-78.71578*T*LN(T)+.0048371295*T**2
    -7.82327E-08*T**3+41752485*T**(-1);  6000 N !
FUNCTION F15856T    298.15  +124152.804-21.0289709*T-20.897*T*LN(T)
    +6.65E-05*T**2-5.58E-09*T**3+3335*T**(-1); 4300 Y
     +104038.336+64.4573272*T-31.558*T*LN(T)+.00230425*T**2
    -8.82333333E-08*T**3+5389360*T**(-1);  8200 Y
     +681283.394-922.574932*T+78.50201*T*LN(T)-.0070638*T**2
    +6.18466667E-08*T**3-5.65175E+08*T**(-1); 10000 N !

FUNCTION GHSERLI    200  -10583.817+217.637482*T-38.940488*T*LN(T)
 +.035466931*T**2-1.9869816E-05*T**3+159994*T**(-1); 453.6 Y
  -559579.123+10547.8799*T-1702.88865*T*LN(T)+2.25832944*T**2
 -5.71066077E-04*T**3+33885874*T**(-1); 500 Y
  -9062.994+179.278285*T-31.2283718*T*LN(T)+.002633221*T**2
 -4.38058E-07*T**3-102387*T**(-1); 3000 N !
FUNCTION GHSERSN  100  -7958.517+122.765451*T-25.858*T*LN(T)
 +5.1185E-04*T**2-3.192767E-06*T**3+18440*T**(-1); 250 Y
  -5855.135+65.443315*T-15.961*T*LN(T)-.0188702*T**2+3.121167E-06*T**3
 -61960*T**(-1); 505.08 Y
  +2524.724+4.005269*T-8.2590486*T*LN(T)-.016814429*T**2
 +2.623131E-06*T**3-1081244*T**(-1)-1.2307E+25*T**(-9); 800 Y
  -8256.959+138.99688*T-28.4512*T*LN(T)-1.2307E+25*T**(-9); 3000 N REF0 !
FUNCTION GHSERZN  298.15  -7285.787+118.470069*T-23.701314*T*LN(T)
-.001712034*T**2-1.264963E-06*T**3; 692.68 Y
  -11070.559+172.34566*T-31.38*T*LN(T)+4.70514E+26*T**(-9); 1700 N REF0 !
FUNCTION GHCPSN  298.15  +3900.0-4.40*T+GHSERSN#; 3000 N REF0 !

FUNCTION GLIQLI  200  +2700.205-5.795621*T+GHSERLI#; 250 Y
 +12015.027-362.187078*T+61.6104424*T*LN(T)-.182426463*T**2
  +6.3955671E-05*T**3-559968*T**(-1); 453.6 Y
 -6057.31+172.652183*T-31.2283718*T*LN(T)+.002633221*T**2-4.38058E-07*T**3
  -102387*T**(-1); 500 Y
 +3005.684-6.626102*T+GHSERLI#; 3000 N REF:0 !
FUNCTION GLIQSN  100  -855.425+108.677684*T-25.858*T*LN(T)
 +5.1185E-04*T**2-3.192767E-06*T**3+18440*T**(-1)+1.47031E-18*T**7; 250 Y
```

```
  +1247.957+51.355548*T-15.961*T*LN(T)-.0188702*T**2+3.121167E-06*T**3
 -61960*T**(-1)+1.47031E-18*T**7; 505.08 Y
  +9496.31-9.809114*T-8.2590486*T*LN(T)-.016814429*T**2
 +2.623131E-06*T**3-1081244*T**(-1); 800 Y
  -1285.372+125.182498*T-28.4512*T*LN(T); 3000 N REF2 !
FUNCTION GLIQZN  298.15  -128.574+108.177079*T-23.701314*T*LN(T)
 -.001712034*T**2-1.264963E-06*T**3-3.58958E-19*T**7; 692.68 Y
  -3620.391+161.608594*T-31.38*T*LN(T); 1700 N REF2 !
FUNCTION GBCTZN  2.98.15  -4398.827+115.959669*T-23.701314*T*LN(T)
-.001712034*T**2-1.264963E-06*T**3; 692.68 Y
  -8183.599+169.83526*T-31.38*T*LN(T)+4.70514E+26*T**(-9); 1700 N REF0 !
FUNCTION GBCCSN  100  +4400-6*T+GHSERSN#; 3000 N REF0 !
FUNCTION GBCCZN   298.15  +2886.96-2.5104*T+GHSERZN#; 6000 N !
FUNCTION GDIASN  100  -9579.608+114.007785*T-22.972*T*LN(T)
 -.00813975*T**2+2.7288E-06*T**3+25615*T**(-1); 298.15 Y
  -9063.001+104.84654*T-21.5750771*T*LN(T)-.008575282*T**2
 +1.784447E-06*T**3-2544*T**(-1); 800 Y
  -10909.351+147.396535*T-28.4512*T*LN(T); 3000 N REF11 !
FUNCTION GFCCLI  200  -10691.817+218.937482*T-38.940488*T*LN(T)
 +.035466931*T**2-1.9869816E-05*T**3+159994*T**(-1); 453.60 Y
  -559687.123+10549.1799*T-1702.88865*T*LN(T)+2.25832944*T**2
 -5.71066077E-04*T**3+33885874*T**(-1); 500 Y
  -9170.994+180.578285*T-31.2283718*T*LN(T)+.002633221*T**2
 -4.38058E-07*T**3-102387*T**(-1); 3000 N REF0 !
 FUNCTION GFCCSN  298.15  -345.135+56.983315*T-15.961*T*LN(T)
 -.0188702*T**2+3.121167E-06*T**3-61960*T**(-1); 505.08 Y
  +8034.724-4.454731*T-8.2590486*T*LN(T)-.016814429*T**2+2.623131E-06*T**3
 -1081244*T**(-1)-1.2307E+25*T**(-9); 800 Y
  -2746.959+130.53688*T-28.4512*T*LN(T)-1.2307E+25*T**(-9); 3000 N REF0 !
FUNCTION GHCPLI  200        -154+2.00*T+GHSERLI#; 3000 N REF0 !
FUNCTION GHCPSN  298.15  +3900.0-4.40*T+GHSERSN#; 3000 N REF0 !

FUNCTION R        100  8.314510; 10000 N !
FUNCTION UN_ASS 298.15 0; 300 N !

TYPE_DEFINITION % SEQ *!
DEFINE_SYSTEM_DEFAULT ELEMENT 2 !
DEFAULT_COMMAND DEF_SYS_ELEMENT VA /- !


PHASE GAS:G %  1  1.0  !
   CONSTITUENT GAS:G :LI,LI2,SN,SN2,ZN :  !

  PARAM G(GAS,LI;0)  298.15 +F12239T#+R#*T*LN(1E-05*P); 6000 N REF6940 !
  PARAM G(GAS,LI2;0) 298.15 +F12319T#+R#*T*LN(1E-05*P); 6000 N REF6966 !
  PARAM G(GAS,SN;0)  298.15 +F15456T#+R#*T*LN(1E-05*P); 6000 N REF8719 !
  PARAM G(GAS,SN2;0) 298.15 +F15470T#+R#*T*LN(1E-05*P); 6000 N REF8729 !
  PARAM G(GAS,ZN;0)  298.15 +F15856T#+R#*T*LN(1E-05*P); 6000 N REF8881 !


PHASE LIQUID:L %  1  1.0  !
   CONSTITUENT LIQUID:L :LI,SN,ZN :  !

  PARAM G(LIQUID,LI;0)  200     +GLIQLI#; 3000 N REF:0 !
  PARAM G(LIQUID,SN;0)  100     +GLIQSN#; 3000 N REF2 !
  PARAM G(LIQUID,ZN;0)  298.15  +GLIQZN#; 6000 N REF0 !
  PAR L(LIQUID,LI,SN;0) 200       -121142.2+24.0000*T; 3000 N REF11 !
  PAR L(LIQUID,LI,SN;1) 200        -87650.9+24.0000*T; 3000 N REF11 !
  PAR L(LIQUID,LI,SN;2) 200         -11383.3-8.7985*T; 3000 N REF11 !
  PAR L(LIQUID,LI,SN;3) 200        +37847.8-37.6298*T; 3000 N REF11 !
  PAR L(LIQUID,LI,ZN;0) 298.15   -45258.58+26.36767*T; 6000 N REF12 !
  PAR L(LIQUID,LI,ZN;1) 298.15   +22887.212-4.19207*T; 6000 N REF12 !
  PAR L(LIQUID,LI,ZN;2) 298.15      -4552.57+4.0715*T; 6000 N REF12 !
```

```
  PAR L(LIQUID,SN,ZN;0) 298.15 +21360.454-97.1651*T+11.4877*T*LN(T);
 6000 N REF10 !
  PAR L(LIQUID,SN,ZN;1) 298.15    -5137.954-0.1805*T+0.5199*T*LN(T);
 6000 N REF10 !
  PAR L(LIQUID,SN,ZN;2) 298.15                          +1716.54532;
 6000 N REF10 !


PHASE AL2LI3  %  2 2   3 !
   CONSTITUENT AL2LI3  :ZN : LI :  !

  PARAM G(AL2LI3,ZN:LI;0)  298.15  +2*GHSERZN#+3*GHSERLI#+15000;
 6000 N REF12 !


PHASE AL4LI9  %  2 4   9 !
   CONSTITUENT AL4LI9  :ZN : LI :  !

  PARAM G(AL4LI9,ZN:LI;0)  298.15  +4*GHSERZN#+9*GHSERLI#+39000;
 6000 N REF12 !


PHASE ALI2M3  %  2 2   3 !
   CONSTITUENT ALI2M3  :LI : LI,ZN :  !

  PARAM G(ALI2M3,LI:LI;0)  298.15 +5*GHSERLI#+19964.61; 6000 N REF12 !
  PARAM G(ALI2M3,LI:ZN;0)  298.15  +2*GHSERLI#+3*GHSERZN#-85329.52
 +30.2362*T; 6000 N REF12 !
  PARAM G(ALI2M3,LI:LI,ZN;0) 298.15 -7720.57+12.5469*T; 6000 N REF12 !
  PARAM G(ALI2M3,LI:LI,ZN;1) 298.15 +1001.18+1.00731*T; 6000 N REF12 !


PHASE ALI2M5  %  2 2   5 !
   CONSTITUENT ALI2M5  :LI,ZN : ZN :  !

  PARAM G(ALI2M5,LI:ZN;0)  298.15  +2*GHSERLI#+5*GHSERZN#
 -123038.907+51.8671*T; 6000 N REF12 !
  PARAM G(ALI2M5,ZN:ZN;0)  298.15   +7*GHSERZN#+12169.34;
 6000 N REF12 !
  PAR L(ALI2M5,LI,ZN:ZN;0)  298.15         -12463.8884; 6000 N REF12 !


PHASE ALIM4  %  2 1   4 !
   CONSTITUENT ALIM4  :LI,ZN : LI,ZN :  !

  PARAM G(ALIM4,LI:LI;0)  298.15     +5*GHSERLI#+15000; 6000 N REF12 !
  PARAM G(ALIM4,ZN:LI;0)  298.15  +GHSERZN#+4*GHSERLI#+78372.0478
 -43.21153*T; 6000 N REF12 !
  PARAM G(ALIM4,LI:ZN;0)  298.15  +GHSERLI#+4*GHSERZN#-78372.0478
 +43.21153*T; 6000 N REF12 !
  PARAM G(ALIM4,ZN:ZN;0)  298.15  +5*GHSERZN#+15000; 6000 N REF12 !
  PAR L(ALIM4,LI,ZN:LI;0) 298.15 -33953.6335+20.1515*T; 6000 N REF12 !
  PAR L(ALIM4,LI:LI,ZN;0) 298.15    -18698.25+7.7695*T; 6000 N REF12 !
  PAR L(ALIM4,ZN:LI,ZN;0) 298.15    -18698.25+7.7695*T; 6000 N REF12 !
  PAR L(ALIM4,LI,ZN:ZN;0) 298.15 -33953.6335+20.1515*T; 6000 N REF12 !


$ THIS PHASE HAS A DISORDERED CONTRIBUTION FROM BCC_A2
PHASE B32  %  3 .5   .5   3 !
   CONSTITUENT B32  :LI,ZN : LI,ZN : VA :  !

  PARA G(B32,LI:LI:VA;0) 298.15                      +0; 6000 N !
  PARAM G(B32,ZN:LI:VA;0) 298.15    -26930.69+10.0062*T; 6000 N REF12 !
```

```
   PARAM G(B32,LI:ZN:VA;0) 298.15    -26930.69+10.0062*T; 6000 N REF12 !
   PARA G(B32,ZN:ZN:VA;0) 298.15                     +0; 6000 N !
   PAR L(B32,LI,ZN:LI:VA;0) 298.15  -26474.38+30.2611*T; 6000 N REF12 !
   PAR L(B32,LI,ZN:LI:VA;1) 298.15  -11635.94+1.40651*T; 6000 N REF12 !
   PAR L(B32,LI:LI,ZN:VA;0) 298.15  -26474.38+30.2611*T; 6000 N REF12 !
   PAR L(B32,LI:LI,ZN:VA;1) 298.15  -11635.94+1.40651*T; 6000 N REF12 !
   PAR L(B32,ZN:LI,ZN:VA;0) 298.15    -13623.42+1.789*T; 6000 N REF12 !
   PAR L(B32,ZN:LI,ZN:VA;1) 298.15    -4786.18-4.0231*T; 6000 N REF12 !
   PAR L(B32,LI,ZN:ZN:VA;0) 298.15    -13623.42+1.789*T; 6000 N REF12 !
   PAR L(B32,LI,ZN:ZN:VA;1) 298.15    -4786.18-4.0231*T; 6000 N REF12 !


 TYPE_DEFINITION & GES AMEND_PHASE_DESCRIPTION B32 DIS_PART BCC_A2,,,!
 PHASE BCC_A2  %&  2 1   3 !
    CONSTITUENT BCC_A2  :LI,ZN : VA :  !

   PARAM G(BCC_A2,LI:VA;0)  200          +GHSERLI#; 3000 N REF:0 !
   PARAM G(BCC_A2,SN:VA;0)  100           +GBCCSN#; 3000 N REF11 !
   PARAM G(BCC_A2,ZN:VA;0)  298.15        +GBCCZN#; 1700 N REF:0 !
$ These next 2 L parameters geenrate a re-entrant bcc in the liq region
$   PAR L(BCC_A2,LI,SN:VA;0) 200     -92821.4-19.3685*T; 3000 N REF11 !
$   PAR L(BCC_A2,LI,SN:VA;1) 200              -79522.7; 3000 N REF11 !
   PAR L(BCC_A2,LI,ZN:VA;0) 298.15  -54260.44+45.772*T; 6000 N REF12 !
   PAR L(BCC_A2,LI,ZN:VA;1) 298.15           +25153.3; 6000 N REF12 !


 PHASE BCT_A5  %  1  1.0  !
    CONSTITUENT BCT_A5  :SN,ZN :  !

   PARAM G(BCT_A5,SN;0)  100                +GHSERSN#; 3000 N REF0 !
   PARAM G(BCT_A5,ZN;0)  298.15              +GBCTZN#; 1700 N REF0 !
   PAR L(BCT_A5,SN,ZN;0) 298.15    +6846.010+24.5560*T; 6000 N REF10 !


 PHASE DIAMOND %  1  1.0  !
    CONSTITUENT DIAMOND :SN :  !

   PARAM G(DIAMOND,SN;0)  200                +GDIASN#; 3000 N REF11 !


 TYPE_DEFINITION ' GES A_P_D FCC_A1 MAGNETIC  -3.0    2.80000E-01 !
 PHASE FCC_A1  %'  2 1   1 !
    CONSTITUENT FCC_A1  :LI,SN,ZN : VA% :  !

$  PARAM G(FCC_A1,LI:VA;0)  200     -108+1.3*T+GHSERLI#; 3000 N REF12 !
   PARAM G(FCC_A1,LI:VA;0)  200       +GFCCLI#; 3000 N REF0 !
   PARAM G(FCC_A1,SN:VA;0)  298.15    +GFCCSN#; 3000 N REF0 !
   PARAM G(FCC_A1,ZN:VA;0)  298.15   +2969.82-1.56968*T+GHSERZN#;
  1700 N REF12 !


 PHASE BLI2M3  %  2 2   3 !
    CONSTITUENT BLI2M3  :LI,ZN : LI,ZN :  !

   PARAM G(BLI2M3,LI:LI;0)  298.15  +5*GHSERLI#+9307.774; 6000 N REF12 !
   PARAM G(BLI2M3,ZN:LI;0)  298.15  +2*GHSERZN#+3*GHSERLI#+84218.37
  -27.758*T; 6000 N REF12 !
   PARAM G(BLI2M3,LI:ZN;0)  298.15  +2*GHSERLI#+3*GHSERZN#-84218.37
  +27.758*T; 6000 N REF12 !
   PARAM G(BLI2M3,ZN:ZN;0)  298.15  +5*GHSERZN#+9307.774; 6000 N REF12 !
   PAR L(BLI2M3,LI,ZN:LI;0) 298.15  -87667.34+59.7976*T; 6000 N REF12 !
   PAR L(BLI2M3,LI,ZN:LI;1) 298.15  +49513.77-70.0108*T; 6000 N REF12 !
   PAR L(BLI2M3,LI:LI,ZN;0) 298.15  +7367.6277+6.9984*T; 6000 N REF12 !
```

```
  PAR L(BLI2M3,LI:LI,ZN;1) 298.15     +8734.917-11.9*T; 6000 N REF12 !
  PAR L(BLI2M3,ZN:LI,ZN;0) 298.15  +7367.6277+6.9984*T; 6000 N REF12 !
  PAR L(BLI2M3,ZN:LI,ZN;1) 298.15     +8734.917-11.9*T; 6000 N REF12 !
  PAR L(BLI2M3,LI,ZN:ZN;0) 298.15  -87667.34+59.7976*T; 6000 N REF12 !
  PAR L(BLI2M3,LI,ZN:ZN;1) 298.15  +49513.77-70.0108*T; 6000 N REF12 !


 PHASE BLI2M5  %  2 2   5 !
    CONSTITUENT BLI2M5  :LI,ZN : ZN :  !

  PARAM G(BLI2M5,LI:ZN;0)  298.15  +2*GHSERLI#+5*GHSERZN#
 -122835.945+51.493182*T; 6000 N REF12 !
  PARAM G(BLI2M5,ZN:ZN;0)  298.15  +7*GHSERZN#+26766; 6000 N REF12 !
  PAR L(BLI2M5,LI,ZN:ZN;0)  298.15       -13440.4616; 6000 N REF12 !
  PAR L(BLI2M5,LI,ZN:ZN;1)  298.15       -21665.1744; 6000 N REF12 !


$ THIS PHASE HAS A DISORDERED CONTRIBUTION FROM HCP_A3
 PHASE BLIM4  %  3 .2   .8   .5 !
    CONSTITUENT BLIM4  :LI,ZN : LI,ZN : VA :  !

  PARAM G(BLIM4,LI:LI:VA;0) 298.15                   +0; 6000 N !
  PAR L(BLIM4,ZN:LI:VA;0)  298.15  +191.117297+.0855478905*T;
 6000 N REF12 !
  PAR L(BLIM4,LI:ZN:VA;0)  298.15  -191.117297-.0855478905*T;
 6000 N REF12 !
  PARA G(BLIM4,ZN:ZN:VA;0) 298.15                    +0; 6000 N !
  PAR L(BLIM4,LI,ZN:LI:VA;0) 298.15   +4904.759-1.9606*T; 6000 N REF12 !
  PAR L(BLIM4,LI,ZN:LI:VA;1) 298.15  -7361.9444+8.2575*T; 6000 N REF12 !
  PAR L(BLIM4,LI:LI,ZN:VA;0) 298.15  +20574.6225-7.41461653*T;
 6000 N REF12 !
  PAR L(BLIM4,LI:LI,ZN:VA;1) 298.15  -29447.7776+33.0299015*T;
 6000 N REF12 !
  PAR L(BLIM4,ZN:LI,ZN:VA;0) 298.15 +19682.1047-7.8141*T; 6000 N REF12 !
  PAR L(BLIM4,ZN:LI,ZN:VA;1) 298.15-29447.7776+33.0299015*T;
 6000 N REF12 !
  PAR L(BLIM4,LI,ZN:ZN:VA;0) 298.15  +5159.5184-1.8466*T; 6000 N REF12 !
  PAR L(BLIM4,LI,ZN:ZN:VA;1) 298.15  -7361.9444+8.2575*T; 6000 N REF12 !


 TYPE_DEFINITION * GES AMEND_PHASE_DESCRIPTION BLIM4 DIS_PART HCP_A3,,,!
 TYPE_DEFINITION ( GES A_P_D HCP_A3 MAGNETIC  -3.0    2.80000E-01 !
 PHASE HCP_A3  %(*  2 1   .5 !
    CONSTITUENT HCP_A3  :LI,SN,ZN% : VA% :  !

  PARAM G(HCP_A3,LI:VA;0)  200  -154+2*T+GHSERLI#; 3000 N REF:0 !
  PARAM G(HC_A3,SN:VA;0)  298.15               +GHCPSN#; 3000 N REF0 !
  PARAM G(HCP_A3,ZN:VA;0)  298.15              +GHSERZN#; 1700 N REF0 !
  PAR L(HCP_A3,LI,ZN:VA;0)  298.15     -29301.52-.2586*T; 6000 N REF12 !
  PAR L(HCP_A3,LI,ZN:VA;1)  298.15    +15702.15+3.5167*T; 6000 N REF12 !
  PAR L(HCP_A3,SN,ZN:VA;0) 298.15  +21310.7476+65.5652*T; 6000 N REF10 !


 PHASE LI22SN5  %  2 22   5 !
    CONSTITUENT LI22SN5  :LI : SN :  !

  PAR G(LI22SN5,LI:SN;0) 200 -1095242.7+270*T+22*GHSERLI#+5*GHSERSN#;
   3000 N REF11 !


 PHASE LI7SN2  %  2 7   2 !
    CONSTITUENT LI7SN2  :LI,SN : SN :  !
```

```
  PAR G(LI7SN2,SN:SN;0) 200 +27000+9*GHSERSN#; 3000 N REF11 !
  PAR G(LI7SN2,LI:SN;0) 200 -383551+81*T+7*GHSERLI#+2*GHSERSN#;
   3000 N REF11 !
  PAR L(LI7SN2,LI,SN:SN;0) 200   +979887.1+9.0115*T; 3000 N REF11 !
  PAR L(LI7SN2,LI,SN:SN;1) 200 -1457538.4+27.5363*T; 3000 N REF11 !


PHASE LI8SN3  %  2 8   3 !
   CONSTITUENT LI8SN3  :LI : SN :  !

  PAR G(LI8SN3,LI:SN;0) 200 -477620.1+90*T+8*GHSERLI#+3*GHSERSN#;
   3000 N REF11 !


PHASE LI13SN5  %  2 13   5 !
   CONSTITUENT LI13SN5  :LI : SN :  !

  PAR G(LI13SN5,LI:SN;0) 200 -780902.1+145*T+13*GHSERLI#+5*GHSERSN#;
   3000 N REF11 !


PHASE LI5SN2  %  2 5   2 !
   CONSTITUENT LI5SN2  :LI : SN :  !

  PAR G(LI5SN2,LI:SN;0) 200 -302420.0+54*T+5*GHSERLI#+2*GHSERSN#;
   3000 N REF11 !


PHASE LI7SN3  %  2 7   3 !
   CONSTITUENT LI7SN3  :LI : SN :  !

  PAR G(LI7SN3,LI:SN;0) 200 -428079.0+75*T+7*GHSERLI#+3*GHSERSN#;
   3000 N REF11 !


PHASE LISN  %  2 1   1 !
   CONSTITUENT LISN  :LI : LI,SN :  !

  PAR G(LISN,LI:SN;0) 200 -73198.3+9.85*T+GHSERLI#+GHSERSN#;
   3000 N REF11 !
  PAR G(LISN,LI:LI;0) 200    +6000+2*GHSERLI#; 3000 N REF11 !
  PAR L(LISN,LI:LI,SN;0) 200         -45169.2; 3000 N REF11 !
  PAR L(LISN,LI:LI,SN;1) 200         +34205.5; 3000 N REF11 !


PHASE LI2SN5  %  2 2   5 !
   CONSTITUENT LI2SN5  :LI : SN :  !

  PAR G(LI2SN5,LI:SN;0) 200 -196683+90*T+2*GHSERLI#+5*GHSERSN#;
   3000 N REF11 !


PHASE LIZN2  %  2 1   2 !
   CONSTITUENT LIZN2  :LI : ZN :  !

  PARAM G(LIZN2,LI:ZN;0)  298.15  +GHSERLI#+2*GHSERZN#-53133.9177
 +23.4265979*T; 6000 N REF12 !


LIST_OF_REFERENCES
NUMBER  SOURCE

  REF0    '  '
```

```
 REF6940 'LI1<G> T.C.R.A.S. Class: 1. LITHIUM <GAS>'
 REF6966 'LI2<G> T.C.R.A.S. Class: 2. LITHIUM <DIATOMIC GAS>'
 REF8719 'SN1<G> T.C.R.A.S. Class: 1. TIN <GAS>'
 REF8729 'SN2<G> T.C.R.A.S. Class: 5.'
 REF8881 'ZN1<G> T.C.R.A.S Class: 1. Data provided by T.C.R.A.S. Oct 1996.'
 REF8715 'SN1 T.C.R.A.S. Class: 6.
       T FUSION revised to be consistent with ITS90. (ATD).'
 REF6932 'LI1 S.G.T.E. ** LITHIUM Data from SGTE Unary DB.'
 REF8875 'ZN1 HULTGREN SELECTED VAL. 1973 SGTE **
       ZINC STANDARD STATE: CODATA KEY VALUE.'
 REF2   'SSOL4.9 (2004-2008): The SGTE General Alloy Solutions Database,
       V4.9f, developed by SGTE (Scientific Group Thermodata Europe), and
       provided by Thermo-Calc Software. '
 REF4   'SSOL4.9 (2004-2008): The SGTE General Alloy Solutions Database,
       V4.9f, developed by SGTE (Scientific Group Thermodata Europe),
       supplemented by GTT, and provided by Thermo-Calc Software.'
 REF9   'Y.-C. Yang, F.-L. Chen, W. Gierlotka, S.-W. Chen, K.-C. Hsieh, and
       L.L.Huang, Thermodynamic properties and phase equilibria of Sn-Bi-Zn
       ternary alloys, Mat. Chem. and Phys. 112, 94-103 (2008).'
 REF10  'Y.-C. Huang, S.-W. Chen, C.-Y. Chou, and W. Gierlotka,
       Liquidus projection and thermodynamic modeling of Sn-Zn-Cu ternary
       system, J. of Alloys and Compounds 477, 283-290 (2009).'
 REF11  'Zhenmin Du, Zhenquan Jiang, and Cuiping Guo, Thermodynamic
       optimizing of the Li-Sn system, Z. für Metallkd. 97, 10-16 (2006).'
 REF12  'Cuiping Guo, Yu Liang, Changrong Li, and Zhenmin Du, Thermodynamic
       description of the Al-Li-Zn system, CALPHAD 35, 54-65 (2011).
        (Li-Zn Binary from Refs. 21).'
 REF21  'Y. Liang, C. Guo, Z. Du, and C. Li, J. All. Compd. 455, 236 (2008).
        (Li-Zn)'
!
```

References

[B1] The Thermo-Calc and DICTRA applications software are products of Thermo-Calc AB; B. Sundman, B. Jansson, and J.-O. Andersson, “The Thermo-Calc Databank System”, CALPHAD **9** (4), 153 (1985); J.-O. Andersson, T. Helander, L. Höglund, Pingfang Shi, and B. Sundman, “THERMO-CALC & DICTRA, computational tools for materials science”, CALPHAD **26** (2), 273-312 (2002); cf. also http://www.thermocalc.se.

[B2] A. Dinsdale, “SGTE Database for Pure Elements”, CALPHAD **15**, 317-425 (1991).

Appendix C. Summary of the thermo-physical properties of Li, Sn and Zn

Appearance	
silvery-white (shown floating in oil) 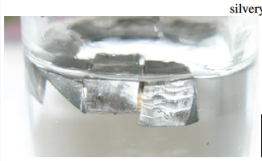 Spectral lines of lithium	
General properties	
Name, symbol, number	lithium, Li, 3
Pronunciation	/ˈlɪθiəm/ *LI-thee-əm*
Element category	alkali metal
Group, period, block	1 (alkali metals), 2, s
Standard atomic weight	6.94(1)
Electron configuration	[He] $2s^1$ 2, 1
History	
Discovery	Johan August Arfwedson (1817)
First isolation	William Thomas Brande (1821)
Physical properties	
Phase	solid
Density (near r.t.)	0.534 g·cm^{-3}
Liquid density at m.p.	0.512 g·cm^{-3}

Melting point	453.65 K, 180.50 °C, 356.90 °F
Boiling point	1615 K, 1342 °C, 2448 °F
Critical point	(extrapolated) 3220 K, 67 MPa
Heat of fusion	3.00 kJ·mol^{-1}
Heat of vaporization	147.1 kJ·mol^{-1}
Molar heat capacity	24.860 J·mol^{-1}·K^{-1}

Vapor pressure

P (Pa)	1	10	100	1 k	10 k	100 k
at T (K)	797	885	995	1144	1337	1610

Atomic properties	
Oxidation states	**+1** (strongly basic oxide)
Electronegativity	0.98 (Pauling scale)
Ionization energies	1st: 520.2 kJ·mol^{-1}
	2nd: 7298.1 kJ·mol^{-1}
	3rd: 11815.0 kJ·mol^{-1}
Atomic radius	152 pm
Covalent radius	128±7 pm
Van der Waals radius	182 pm
Miscellanea	
Crystal structure	body-centered cubic
Magnetic ordering	paramagnetic
Electrical resistivity	(20 °C) 92.8 nΩ·m
Thermal conductivity	84.8 W·m^{-1}·K^{-1}
Thermal expansion	(25 °C) 46 µm·m^{-1}·K^{-1}
Speed of sound (thin rod)	(20 °C) 6000 m·s^{-1}
Young's modulus	4.9 GPa
Shear modulus	4.2 GPa
Bulk modulus	11 GPa
Mohs hardness	0.6
CAS registry number	7439-93-2
Most stable isotopes	
Main article: Isotopes of lithium	

Appearance	
silvery (left, beta) or gray (right, alpha) 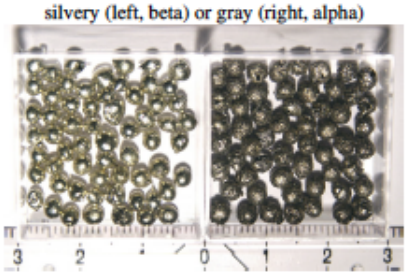	
General properties	
Name, symbol, number	tin, Sn, 50
Pronunciation	/ˈtɪn/
Element category	poor metal
Group, period, block	14, 5, p
Standard atomic weight	118.710
Electron configuration	[Kr] $4d^{10}\,5s^2\,5p^2$ 2, 8, 18, 18, 4
History	
Discovery	around 3500 BC
Physical properties	
Phase	solid
Density (near r.t.)	(white) 7.365 g·cm^{-3}
Density (near r.t.)	(gray) 5.769 g·cm^{-3}
Liquid density at m.p.	6.99 g·cm^{-3}
Melting point	505.08 K, 231.93 °C, 449.47 °F
Boiling point	2875 K, 2602 °C, 4716 °F
Heat of fusion	(white) 7.03 kJ·mol^{-1}
Heat of vaporization	(white) 296.1 kJ·mol^{-1}
Molar heat capacity	(white) 27.112 J·mol^{-1}·K^{-1}

Vapor pressure

P (Pa)	1	10	100	1 k	10 k	100 k
at T (K)	1497	1657	1855	2107	2438	2893

Atomic properties	
Oxidation states	**4**, 3, 2, 1, -4 (amphoteric oxide)
Electronegativity	1.96 (Pauling scale)
Ionization energies	1st: 708.6 kJ·mol^{-1}
	2nd: 1411.8 kJ·mol^{-1}
	3rd: 2943.0 kJ·mol^{-1}
Atomic radius	140 pm
Covalent radius	139±4 pm
Van der Waals radius	217 pm
Miscellanea	
Crystal structure	tetragonal 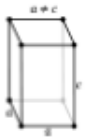 white
	diamond cubic gray
Magnetic ordering	(gray) diamagnetic[1], (white) paramagnetic
Electrical resistivity	(0 °C) 115 nΩ·m
Thermal conductivity	66.8 W·m^{-1}·K^{-1}
Thermal expansion	(25 °C) 22.0 µm·m^{-1}·K^{-1}
Speed of sound (thin rod)	(r.t.) (rolled) 2730 m·s^{-1}
Young's modulus	50 GPa
Shear modulus	18 GPa

Appearance	
silver-gray 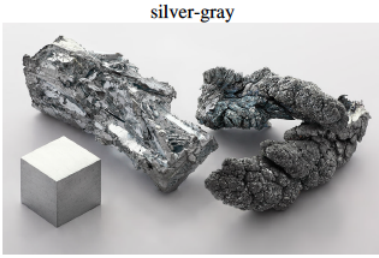	
General properties	
Name, symbol, number	zinc, Zn, 30
Pronunciation	/ˈzɪŋk/ ***ZINGK***
Element category	transition metal alternatively considered a post-transition metal
Group, period, block	12, 4, d
Standard atomic weight	65.38(2)
Electron configuration	[Ar] $3d^{10}\,4s^2$ 2, 8, 18, 2
History	
Discovery	Indian metallurgists (before 1000 BC)
First isolation	Andreas Sigismund Marggraf (1746)
Recognized as a unique metal by	Rasaratna Samuccaya (800)
Physical properties	
Phase	solid

Density (near r.t.)	7.14 g·cm^{-3}
Liquid density at m.p.	6.57 g·cm^{-3}
Melting point	692.68 K, 419.53 °C, 787.15 °F
Boiling point	1180 K, 907 °C, 1665 °F
Heat of fusion	7.32 kJ·mol^{-1}
Heat of vaporization	123.6 kJ·mol^{-1}
Molar heat capacity	25.470 J·mol^{-1}·K^{-1}

Vapor pressure

P (Pa)	1	10	100	1 k	10 k	100 k
at T (K)	610	670	750	852	990	1179

Atomic properties	
Oxidation states	**+2**, +1, 0 (amphoteric oxide)
Electronegativity	1.65 (Pauling scale)
Ionization energies (more)	1st: 906.4 kJ·mol^{-1}
	2nd: 1733.3 kJ·mol^{-1}
	3rd: 3833 kJ·mol^{-1}
Atomic radius	134 pm
Covalent radius	122±4 pm
Van der Waals radius	139 pm
Miscellanea	
Crystal structure	hexagonal close-packed
Magnetic ordering	diamagnetic
Electrical resistivity	(20 °C) 59.0 nΩ·m
Thermal conductivity	116 W·m^{-1}·K^{-1}
Thermal expansion	(25 °C) 30.2 µm·m^{-1}·K^{-1}
Speed of sound (thin rod)	(r.t.) (rolled) 3850 m·s^{-1}
Young's modulus	108 GPa
Shear modulus	43 GPa
Bulk modulus	70 GPa
Poisson ratio	0.25
Mohs hardness	2.5
Brinell hardness	412 MPa
CAS registry number	7440-66-6

Appendix D. Other potential elements that could lead to low melting point alloys when mixed with Li

Au, Ba, Ca, Ga, Sr, Zn

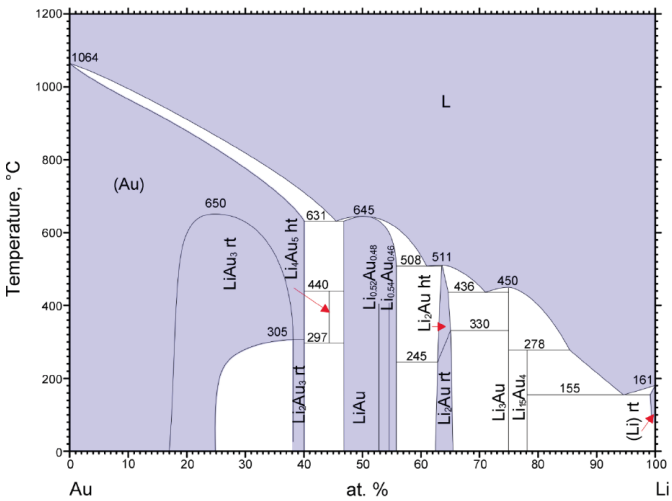

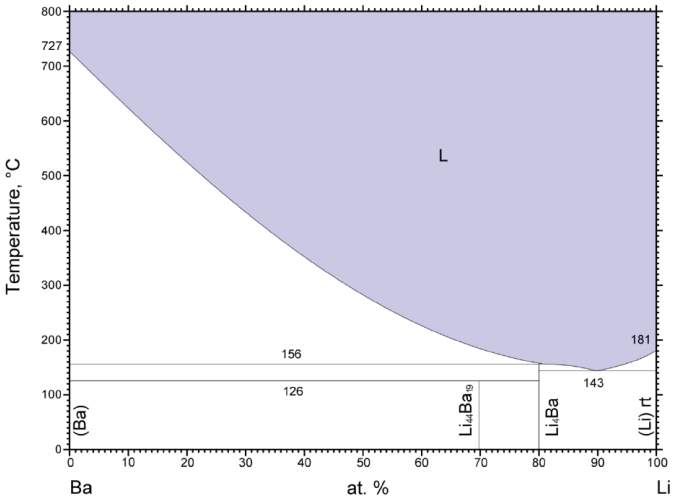

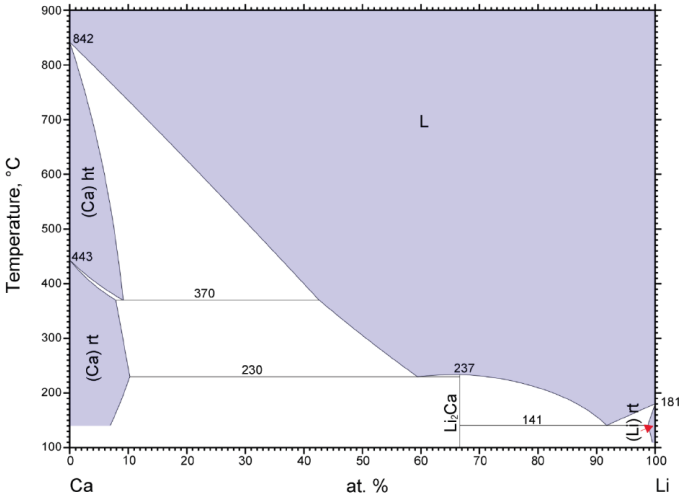

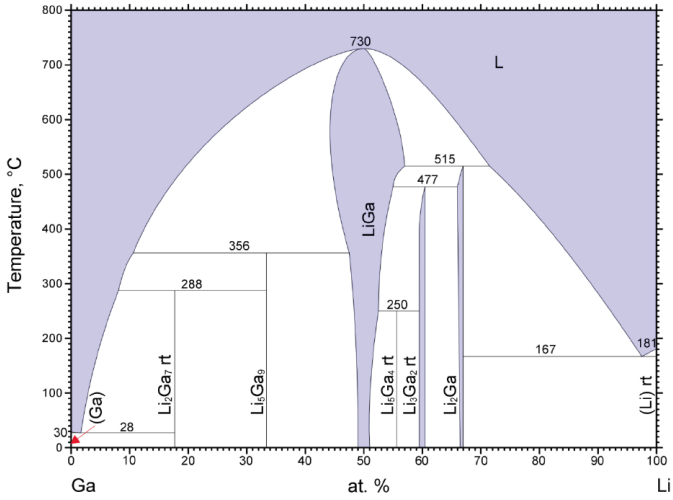

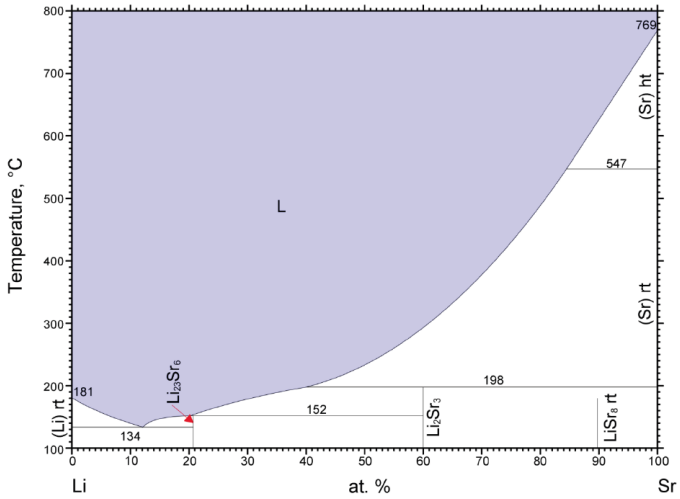

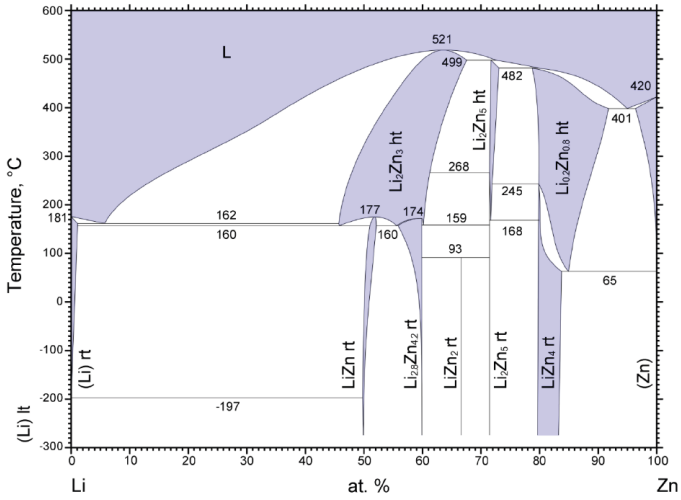

and to some extent

In, Mg, Na, Pd, Sb, and Sn

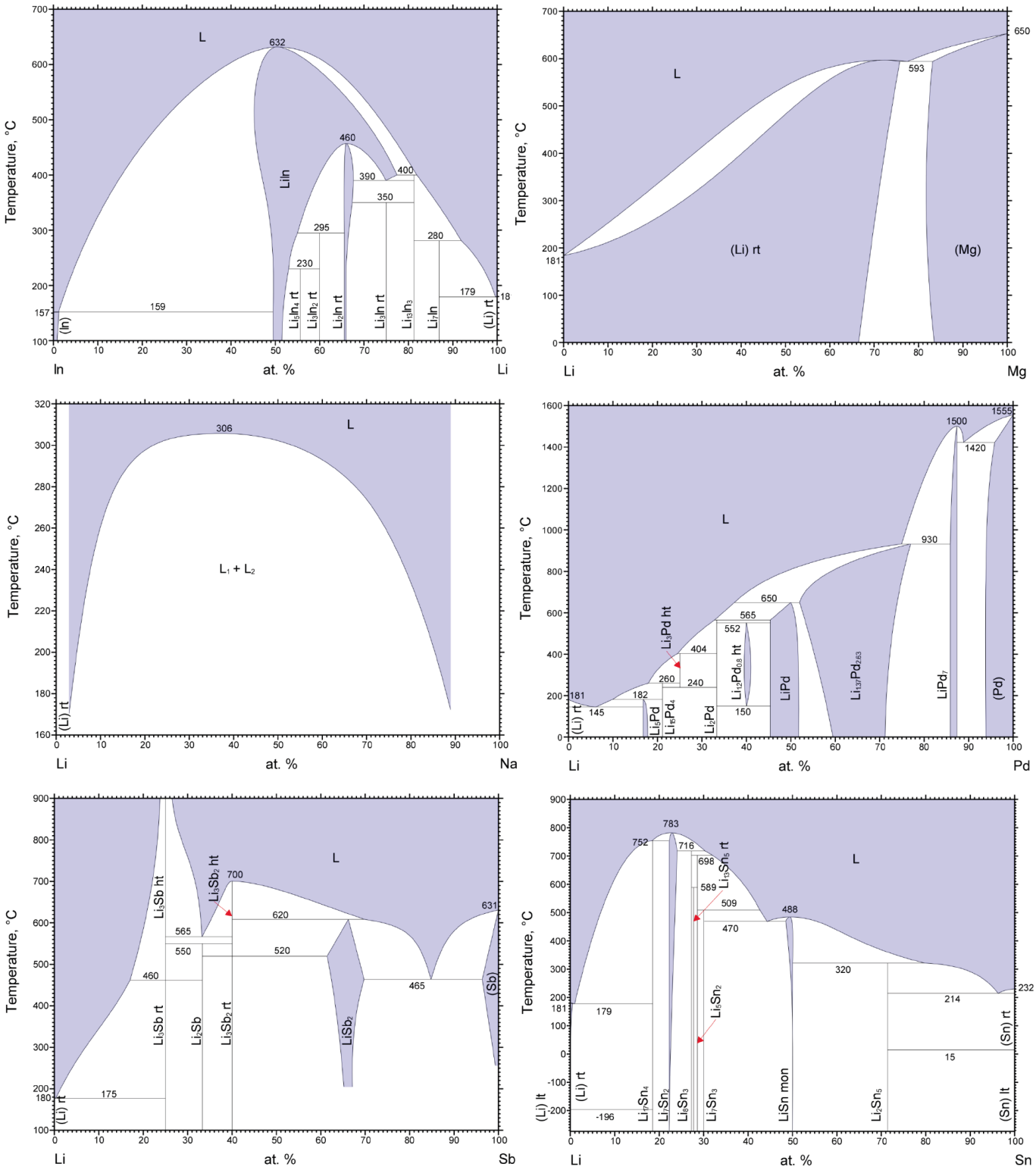

in replacement of the commonly used binary Li-Pb system

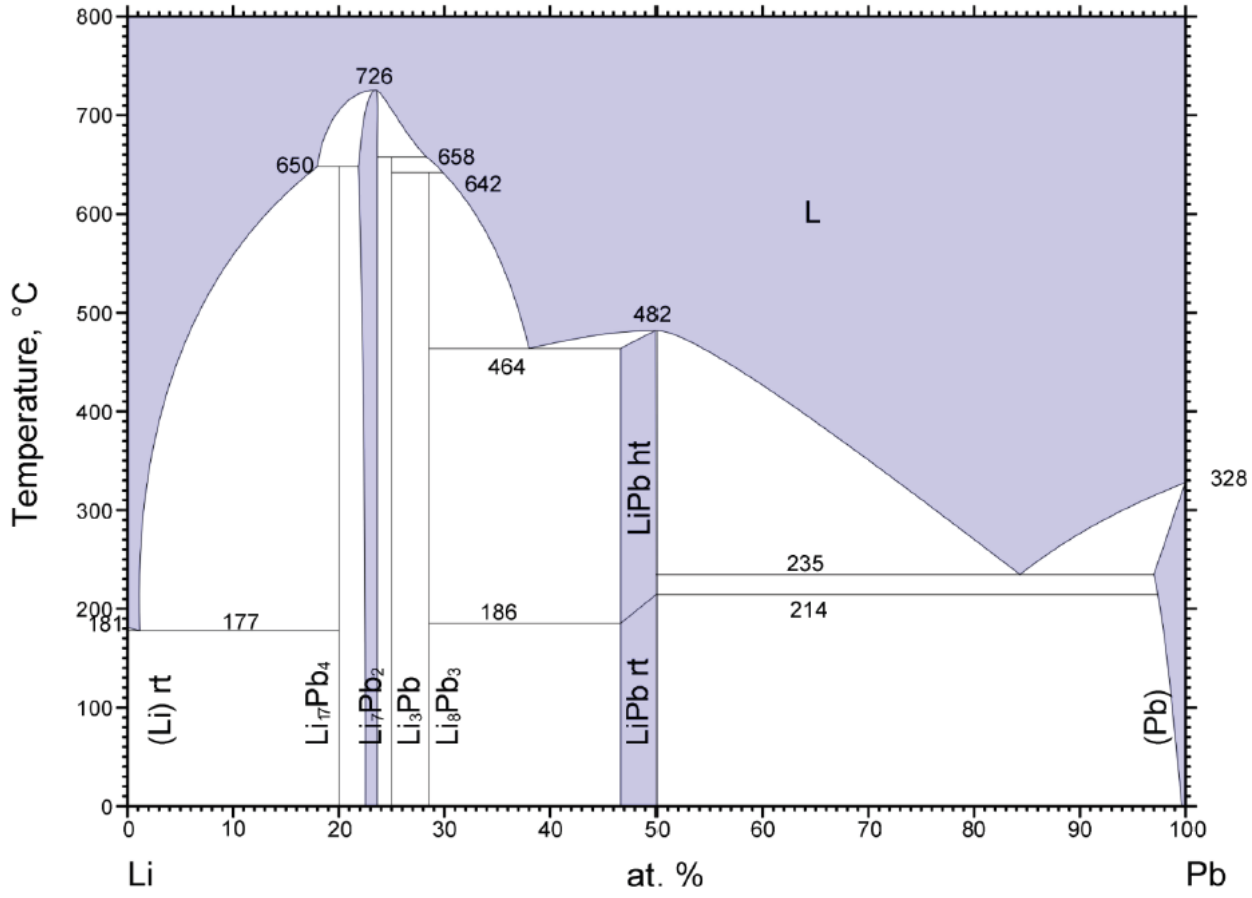

N. B.: Other thermodynamically assessed systems that may be relevant for this work

	Ag	Al	Bi	Cu	Ga	In	Li	Na	Si	Sn	Ti	Zn
Ag												
Al												
Bi												
Cu												
Ga												
In												
Li												
Na												
Si												
Sn												
Ti												
Zn												

Al-Li
N. Saunders, CALPHAD **1**, 237 (1977).
J. Gröbner, H.-L. Lukas, and F. Aldinger, CAPHAD **20** (2), 247-254 (1996).
N. Saunders, Z. Metallkd. **80**, 894-903 (1989). (first assessment)
B. Hallstedt and O. Kim, Z. für Metllkde. **98**, 961 (2007).

Al-Sn
X.J. Liu, I. Ohnuma, C.P. Wang, M. Jiang, R. Kainuma, K. Ishida, M. Ode, T. Koyama, H. Onodera, and T. Suzuki, "Thermodynamic Database on Microsolders and Copper-Based Alloy Systems", J. Electron. Mater. **32** (11), 1265-1272 (2003).

Al-Zn
M. Mathon, K. Jardet, E. Aragon, et al., CALPHAD **24**, 253 (2000).

Cu-Sn
Wojcieh Gierlotka**, "**Thermodynamic description of the Cu–Sn system", J. Mater. Res. **22** (11), 3158-3165 (2007).

Cu-Zn
Wojcieh Gierlotka**, "**Thermodynamic description of the Cu–Zn system", J. Mater. Res. **23** (1), 258-263 (2008).

Li-Si
H. Okamoto, "The Li-Si system", Bull. Alloy Phase Diagrams **11**, 306-312 (1990).
V. L. Chevriera, J. W. Zwanzigerb, J. R. Dahna, "First principles study of Li–Si crystalline phases: Charge transfer, electronic structure, and lattice vibrations", J. of Alloys and Compounds **496**, 25-36 (2010).

Li-Sn
Zhenmin Du, Zhenquan Jiang, and Cuiping Guo, "Thermodynamic optimizing of the Li-Sn system", Z. für Metallkd. **97**, 10-16 (2006).
D. Henriques, V. Motalov, L. Bencze, S. Fürtauer, and T. Markus, "Experimental thermodynamics of the Li-Sn system by Knudsen Effusion Mass Spectrometry", J. of Alloys and Compounds **585**, 299-306 (2014).

Li-Zn
Yu Liang, Zhenmin Du, Cuiping Guo, and Changrong Li, "Thermodynamic Modeling of the Li-Zn System", J. of Alloys and Compounds **455**, 236-242 (2008).

Sn-Zn
H. Ohtani, M. Miyashita, and K. Ishida, "Thermodynamic study of phase equilibria in the Sn-Ag-Zn system", J. Jpn. Inst. Metals **63** (6), 685-694 (1999).

K. Doi, S. Ono, H. Ohtani, and M. Hasebe, "Thermodynamic Study of the Phase equilibria in the Sn-Ti-Zn Ternary System", J. of Phase Equilibria and Diffusion **27** (1), 63-74 (2006).
Jiri Vizdal, Maria Helena Braga, Ales Kroupa, Klaus W. Richter, Delfim Soares, Luís Filipe Malheiros, and Jorge Ferreira, "Thermodynamic assessment of the Bi–Sn–Zn System", CALPHAD **31**, 438-448 (2007).
Ching-feng Yang, Feng-ling Chen,Wojciech Gierlotka, Sinn-wen Chen, Ker-chang Hsieh, and Li-ling Huang, "Thermodynamic properties and phase equilibria of Sn–Bi–Zn ternary alloys", Mater. Chem. and Phys. **112**, 94-103 (2008).
Yu-chih Huang, Sinn-wen Chen, Chin-yi Chou, and Wojciech Gierlotka, "Liquidus projection and thermodynamic modeling of Sn–Zn–Cu ternary system", J. of Alloys and Compounds **477**, 283-290 (2009).

Ag-Sn-Zn

H. Ohtani, M. Miyashita, and K. Ishida, "Thermodynamic study of phase equilibria in the Sn-Ag-Zn system", J. Jpn. Inst. Metals **63** (6), 685-694 (1999).
G. Vassilev, V. Gandova, N. Milcheva, and G. Wnuk, "Thermodynamic description of the system Ag-Sn-Zn", CALPHAD **43**, 133-138 (2013) (and database).

Al-Bi-Sn

H. X. Liu, C. P. Wang, Y. Yu, X.J. Liu, Y. Takaku, I. Ohnuma, R. Kainuma, and K. Ishida, "Experimental investigation and thermodynamic calculation of the phase equilibria in the Al-Bi-Sn ternary system", J. of Phase Equil. and Diff. **33** (1), 9-19 (2012).

Al-Ga-Zn

M. Mathon, K. Jardet, E. Aragon, P. Satre, and A. Sebaoun, "Reassessments of the Three Binary Systems and Discussion on Possible Estimations and on Optimisation of the Ternary System", CALPHAD **24** (3), 253-284 (2000).

Al-Li-Si

J. Gröbner, D. Kevorkov, and R. Schmid-Fetzer, "The Al-Li-Si System – 2. Experimental Study and Thermodynamic Calculation of the Polythermal Equilibria", J. of Sol. State Chem. **156**, 506-511 (2001).

Al-Li-Zn

Cuiping Guo, Yu Liang, Changrong Li, and Zhenmin Du, "Thermodynamic description of the Al–Li–Zn system", CALPHAD **35**, 54-65 (2011).

Bi-Pb-Sn

Seung Wook Yoon and Hyuck Mo Lee, "A thermodynamic study of phase equilibria in the Sn-Bi-Pb solder system", CALPHAD 22 (2), 167-178 (1998).

Bi-Sn-Zn

Jiri Vizdal, Maria Helena Braga, Ales Kroupa, Klaus W. Richter, Delfim Soares, Luís Filipe Malheiros, and Jorge Ferreira, "Thermodynamic assessment of the Bi–Sn–Zn System",

CALPHAD **31**, 438-448 (2007).
M. H. Braga, J. Vizdal, A. Kroupa, J. Ferreira, D. Soares, L. F. Malheiros, "The experimental study of the Bi–Sn, Bi–Zn and Bi–Sn–Zn systems", CALPHAD **31**, 468-478 (2007).
Ching-feng Yang, Feng-ling Chen,Wojciech Gierlotka, Sinn-wen Chen, Ker-chang Hsieh, and Li-ling Huang, "Thermodynamic properties and phase equilibria of Sn–Bi–Zn ternary alloys", Mater. Chem. and Phys. **112**, 94-103 (2008).

Cu-In-Sn

Dominika Jendrzejczyk-Handzlik, Wojciech Gierlotka, and Krzysztof Fitzner, "Thermodynamic properties of liquid copper–indium–tin alloys determined from e.m.f. measurements", J. Chem. Thermodynamics **41**, 2560-256 (2009).

Cu-Sb-Sn

Sinn-wen Chen, An-ren Zi, Wojciech Gierlotka, Ching-feng Yang, Chao-hong Wang, Shih-kang Lin, and Chia-ming Hsu, "Phase equilibria of Sn–Sb–Cu system", Mater. Chem. and Phys. **132**, 703-715 (2012).

Cu-Sn-Zn

T. Jantzen and P. J. Spencer, "Thermodynamic assessments of the Cu-Pb-Zn and Cu-Sn-Zn systems", CALPHAD **22** (3), 417-434 (1998).
Yu-chih Huang, Sinn-wen Chen, Chin-yi Chou, and Wojciech Gierlotka, "Liquidus projection and thermodynamic modeling of Sn–Zn–Cu ternary system", J. of Alloys and Compounds **477**, 283-290 (2009).

In-Ni-Sn

C. Schmetterer, A. Zemanova, H. Flandorfer, A. Kroupa, and H. Ipser, "Phase equilibria in the ternary In-Ni-Sn system at 700 ^{o}C", Intermetallics **35**, 90-97 (2013).

In-Sb-Sn

Dragan Manasijevíc, Jan Vrestál, Dusko Miníc, Ales Kroupa, Dragana Zivkovíc, and Zivan Zivkovíc, "Experimental investigation and thermodynamic description of the In–Sb–Sn ternary system", J. of Alloys and Compounds **450**, 193-199 (2008).

In-Sn-Zn

Y. Cui, X.J. Liu, I. Ohnuma, R. Kainuma, and H. Ohtani, K. Ishida, "Thermodynamic calculation of the In–Sn–Zn ternary system", J. of Alloys and Compounds **320**, 234-241 (2001).

Li-Pb-X (X=Cr, Fe, Ni)

Stéphane Gossé, "Thermodynamic assessment of solubility and activity of iron, chromium, and nickel in lead bismuth eutectic", J. of Nucl. Mater. **449**, 122-131 (2014).

Sn-Ti-Zn

K. Doi, S. Ono, H. Ohtani, and M. Hasebe, "Thermodynamic Study of the Phase equilibria in the Sn-Ti-Zn Ternary System", J. of Phase Equilibria and Diffusion **27** (1), 63-74 (2006).